Journal of African Earth Sciences 161 (2020) 103665

Contents lists available at ScienceDirect

Journal of African Earth Sciences

journal homepage: www.elsevier.com/locate/jafrearsci

Characterisation of groundwater flow and recharge in crystalline basement rocks in the Talensi District, Northern Ghana

Bismark Awinbire Akurugu, Larry Pax Chegbeleh*, Sandow Mark Yidana

Department of Earth Science, Box LG. 58, University of Ghana, Legon, Accra, Ghana

ARTICLE INFO

Keywords:
Groundwater
Hydraulic conductivity
Isotopes
Numerical modelling
Recharge
Talensi

ABSTRACT

A numerical groundwater flow model, calibrated under equilibrium conditions to characterise the spatial variation of key hydraulic parameters and groundwater flow pattern in a crystalline aquifer in the Upper East Region of Ghana has been developed. The development of groundwater flow model was to provide the baseline information to assist in assessing the impacts of population growth and climate change scenarios on large scale development of groundwater resources for various uses. The results revealed an apparent dominant northeast–southwest flow pattern influenced mainly by the hydraulic conductivity field, with estimated values ranging between 0.001 and 58 m/day, and local flow systems which are controlled mainly by local variations in the topography in the area. The estimated average groundwater recharge from the calibrated model and chloride mass balance technique: 2.00% and 2.07% of the annual precipitation respectively has a direct positive correlation with elevation. The low recharge rate is evident in the high evaporation rates as revealed by stable isotope (δ^2H and $\delta^{18}O$) analysis of sampled water sources. The study also reveals the aquifer is being partly recharged by the White Volta River. This gives an indication that the area holds good groundwater fortunes for potential commercial groundwater development as predicted by scenario analysis which suggests that the aquifer can sustain increased abstractions by more than 100% of the current rate provided the current recharge rate is maintained. However, for the aquifer to sustain large scale abstractions beyond 100% of the current rate under conditions of reduced vertical recharge by more than 40% of the current rate, deliberate efforts would have to be made to enhance artificial vertical recharge to augment the natural recharge.

1. Introduction

Groundwater has proven to be a reliable source of water supply for domestic, industrial and irrigation purposes especially in times of varying precipitation patterns and related increased water demands during droughts, and periods of depleted surface water sources. Economic growth, industrialisation and climate variability are intensely affecting the availability of water supply worldwide. These conditions have been predicted to worsen especially in arid and semi-arid countries (Lloyd's 360° Risk Insight, 2010). The consumption of water worldwide increases yearly while most of the world's water resources continue to dwindle due to improper environmental management practices.

Groundwater is considered to be a vital source of water supply for about a third of the world's population (FAO, 2017). In Ghana, about 70% of the population depends on groundwater for various purposes (Kortatsi et al., 2007), whereas about 25% of the urban communities and 90% of the rural folks heavily depend on groundwater for their household water requirements (Yankey et al., 2011). The availability of quality water in sufficient quantities for domestic, agricultural and industrial purposes is key to the development of any nation. Ghana as a developing country is challenged with the problem of providing adequate quality water to meet the demand of its populace. Northern Ghana where poverty and a short rainy season regime are dominant is severely affected by the lack of adequate quality water supply. Also, surface water sources in such areas are less available and easily run dry during long dry seasons, as such most institutions place emphasis on well-siting techniques to meet the potable water requirements of communities in these areas (UNDP, 2019). Groundwater sources have become the preferred means of supplying water to meet the growing demand of the largely rural and dispersed communities and small urban towns in the country mainly due to its slow response to changing rainfall patterns (Saana et al., 2016), protection from microbial contamination and to some extent massive pollution. It is also relatively cheap to develop and easily site close to the demand centres (UNEP, 2002), hence making it demand responsive and appropriate for

* Corresponding author.
E-mail addresses: lpchegbeleh@ug.edu.gh, larrypax@yahoo.com (L.P. Chegbeleh).

https://doi.org/10.1016/j.jafrearsci.2019.103665
Received 27 April 2019; Received in revised form 27 August 2019; Accepted 7 October 2019
Available online 09 October 2019
1464-343X/

participatory approaches to dealing with most sanitation and rural water programmes.

The unplanned development and over-exploitation of groundwater resources in some portions of the country have elevated the concern and necessity for cautious and scientific resource management and conservation. An understanding of aquifer parameters such as recharge rate, hydraulic conductivity, hydraulic head distribution, specific capacity and aquifer depths are very important in characterising groundwater systems and for the management of the resource. Although groundwater is not easily accessible, numerous techniques have been employed with the aim of investigating aquifer hydraulic properties to locate groundwater supplies and to delineate likely zones of low borehole success rates. A traditional method of estimating aquifer hydraulic parameters, such as specific yield and hydraulic conductivity, is the pumping test method (Bateni et al., 2015; Das et al., 2017). Although this method gives a good estimate of aquifer hydraulic properties, drilling of pumping and observation boreholes over a domain has proven to be very expensive and time consuming (Bateni et al., 2015; Das et al., 2017). Also, pumping test only provides point estimates of the hydraulic parameters and does not give detailed information of the spatial distribution of the hydraulic parameters of the site being characterised (Slater, 2002; Yidana et al., 2015). Similarly, tracer test has also been used in the determination of aquifer hydraulic parameters although results obtained are only approximations due to field limitations (Todd and Mays, 2005).

Hence, an alternative approach to characterising regional hydrogeological conditions and the sparse spatial distribution and behaviour of aquifer hydraulic parameters is through stratigraphic description and numerical simulation (Yidana and Chegbeleh, 2013). Given sufficient data, application of groundwater models is more economical and provide reliable information on the variety of aquifer hydraulic properties as compared to conventional pumping test which provides point data on aquifer properties (Yidana and Chegbeleh, 2013). Rising water demands and uneven rainfall variability as a result of global climatic conditions and associated increased abstraction rates leading to the depletion of groundwater sources in some portions of the study area in recent times (Gyau-Boakye, 2001; Obuobie et al., 2012) has necessitated the need to properly characterise the hydraulic properties of the domain to aid policy makers and stakeholders in the management of the groundwater resource to meet growing needs and sustainability of the resource.

Talensi District is characterised by a typical rural water supply system comprising mainly of boreholes and hand dug wells and other natural water bodies such as dammed reservoirs, rivers and dug outs. Groundwater resources contribute significantly to the socio-economic activities such as water supply and sanitation, industry, agriculture, urban development and research among others in the district (Talensi District Assembly, 2014). This study, therefore characterised the spatial distribution of key hydraulic parameters and groundwater flow geometry of the aquifer system in the area. This was to provide the initial baseline information to assist in assessing the impacts of population growth and climate change scenarios on large scale development of groundwater resources for various uses. This will offer a great opportunity to improve agriculture, food security and livelihoods of indigents in the district, and by extension will reduce rural-urban migration.

2. Study area

Talensi District is located in the Upper East Region of Ghana. It is bordered to the north by Bolgatanga Municipal, south by the West and East Mamprusi Districts, Kassena-Nankana District to the west and the Bawku West District to the east. It falls within the boundaries of latitudes $10^0 35''$ and $10^0 60''$ north and longitudes $0^0 31''$ and $1^0 05''$ west (Fig. 1). It has a total population of 81,194 people of which about 90% are peasant farmers, and a land mass of 912 km^2 (Talensi District Assembly, 2014). The district lies in the savanna zone, which is subdivided into Sudan, Sahel and Guinea-Savanna zones (Fagariba et al., 2018). The domain experiences semi-arid conditions, with unimodal rainy season (Fagariba et al., 2018; Talensi District Assembly, 2014). The district has two main seasons; a rainy season, which is irregular, and runs from May to October, characterised by short intense rains preceded by heavy storms, and a prolonged dry season that stretches from October to April with barely any rains (Talensi District Assembly, 2014). The monthly rainfall ranges between 88 mm and 110 mm with an annual mean rainfall of 980 mm. The area experiences a maximum temperature of 45 °C in March and April, and a minimum of 12 °C in December. Relative humidity is highest during the rainy season with an average value of 65%. It drops rapidly after the end of the rainy season in October, reaching a low of less than 10% during the harmattan period in December and January (Martin, 2006). Monthly rainfall only exceeds potential evapotranspiration in the three wettest months July, August and September.

The vegetation of the district is a typical guinea savannah woodland; comprising mainly of short widely spread plants and shrubs, which usually shed foliage at the end of the growing season, and trees and ground flora of grass, which get burnt by fire or the scorching sun during the long dry season (Talensi District Assembly, 2014). Typical trees are dawadawa, shea trees, acacias and baobab. These conditions impact negatively on rainfall amount in the area, thereby affecting the amount of groundwater. As a predominantly agricultural economy, the excessive temperatures and long dry season periods compel indigents to seek alternative livelihoods elsewhere, usually southern Ghana, in order to cater for the food gap during those periods; this has a tendency of drawing the young and energetic farm labour from the communities (Talensi District Assembly, 2014).

2.1. Geology and hydrogeology

About 75% of the landmass of the district is underlain by crystalline Precambrian rocks of the Birimian Supergroup, which occur in the central, southern and western parts with associated granitoid intrusions and a remote patch of the Tarkwaian series around the eastern portion of the district (Boateng, 1959), whilst the Voltaian Supergroup, Kwahu-Bombouaka Group underlie the southeastern portions of the district (Fig. 2). Gyau-Boakye and Tumbulto (2006), indicated that the Birimian system consists of gneiss, phyllite, schist, migmatite, granite-gneiss and quartzite. The Birimian Supergroup is the dominant rock formation in the district and comprises of volcanoclastics, basaltic flows, cherts and hornblende. It is intruded by K-feldspar-rich granitoids, mainly granite and monzonite (Bongo type), of the Eburnean Plutonic suite. The granitoids are of uncertain age and believed to be post-Birimian and pre-Tarkwaian age (Abdul-Ganiyu and Gbedzi, 2015; Junner and Hirst, 1946; Kesse, 1985). The Voltaian Supergroup, Kwahu-Bombouaka Group underlying the lower portions of the district are composed mainly of fine-grained micaceous sandstones, medium grained mudstones and shales. They overlie the Birimian and Tarkwaian in the district, and are thought to be of late Precambrian to Paleozoic age. The Voltaian Supergroup is subdivided into three main stratigraphic units based on lithology and field relationships; Basal sandstones, Oti/Pendjari and Obosum supergroups. The Basal sandstones comprises quartz sandstone formation of about 75 m thick and commonly occur along the northern and western edges of the Voltaian Supergroup. The Oti/Pendjari on the other hand is much thicker (1500 m–4000 m) and comprises argillaceous sandstones, arkose, siltstones, interbedded mudstone, sandy shale and conglomerates (Carney et al., 2008). The Obosum formation of the Voltaian Supergroup consists of dirty-yellow, fine-grained, thinly bedded, micaceous feldspathic quartz sandstones with subordinate argillite intercalations and whitish-yellow, massive, fine to medium-grained, cross-bedded arkosic and quartzose sandstones.

The district is underlain partly by the Basement Complex comprising Precambrian crystalline igneous and metamorphic rocks, mainly

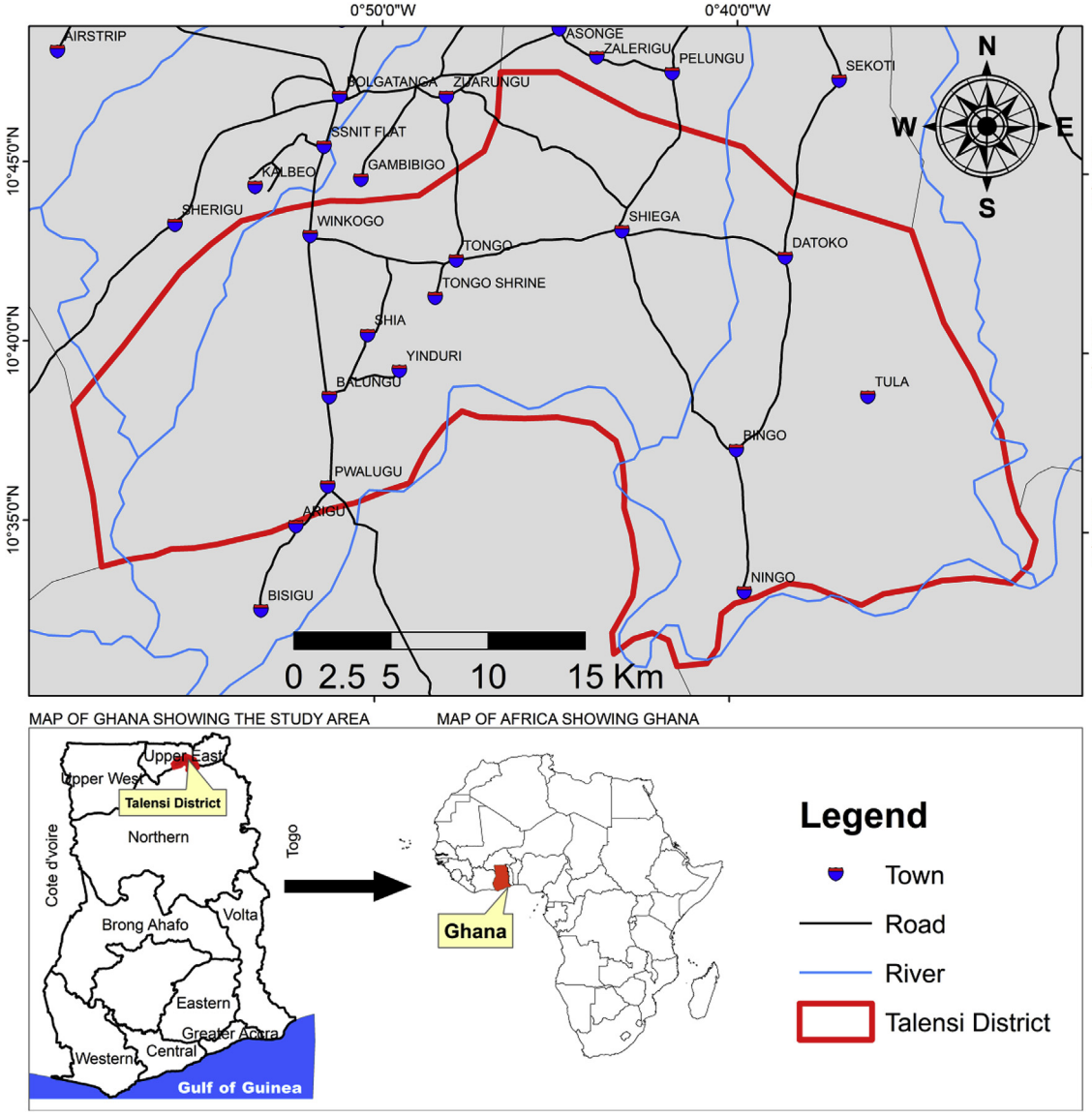

Fig. 1. Location map of the study area.

the Birimian, granites and Tarkwaian, and Paleozoic Consolidated Sedimentary formation, mainly the Voltaian system (Dapaah-Siakwan and Gyau-Boakye, 2000; Kortatsi, 1994), which consist of sandstones, mudstones, limestones, arkose and shales. The Birimian and Tarkwaian comprise gneiss, granite, phyllite, migmatite and schist. The rocks of the Basement Complex and the Voltaian system are impermeable, characterised essentially by little or no primary porosity. However, groundwater occurrence in these formations is associated with the occurrence of secondary porosities caused by fracturing, faulting, jointing, shearing and weathering (WRC, 2011). Aquifers in the study area are generally semi-confined and structurally controlled due to the development of fractures, thus giving rise to secondary permeability (Dapaah-Siakwan and Gyau-Boakye, 2000). Two main types of aquifers in the district can be identified: the weathered zone aquifers and the fractured zone aquifers. The weathered zone aquifers usually occur at the base of the thick weathered layer while the fractured zone aquifers usually occur at some depth beneath the weathered zone (Kortatsi, 1994; WRC, 2011).

Borehole yields within the weathered zone depends on the amount of rainfall, such that where there is less amount of rainfall, no fractures and a thin depth of weathering, groundwater potential is very low or virtually non-existent. Borehole yield within the weathered zone usually range from 0.41 m^3/hr to 29.8 m^3/hr (Dapaah-Siakwan and Gyau-Boakye, 2000). Whereas yields in the fractured zones range between 1 m^3/hr to 9 m^3/hr, but hardly exceed 6 m^3/hr according to Dapaah-Siakwan and Gyau-Boakye (2000). Wardrop (1980) stated that analysis of the available hydrogeological and lithological data from wells drilled within the basin indicates that fractured aquifer provides most of the wells with water. Hence the nature, aperture and degree of interconnection between joints determine the hydrogeological fortunes of the rocks within the study area.

3. Materials and methods

3.1. Data collection and analyses

Both primary and secondary data were used in this study. The secondary hydrogeological data collected for this study included borehole logs and pumping test data. These were obtained from the head office of Community Water and Sanitation Agency (CWSA), Accra. Analyses of the pumping test data using the Cooper-Jacob method (Cooper and Jacob, 1946) resulted in the estimation of some key hydraulic parameters: hydraulic conductivity (K) and transmissivity (T). The estimated parameters served as inputs during numerical

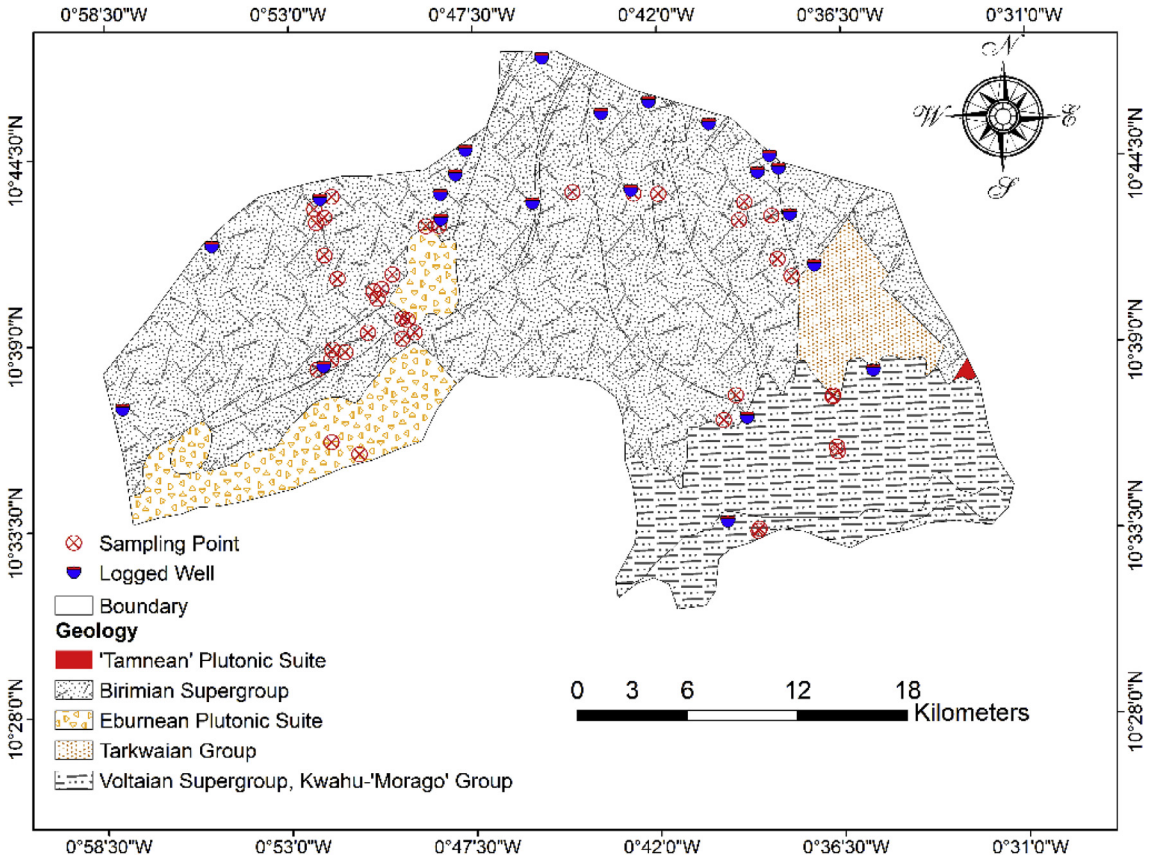

Fig. 2. Geological map of the study area.

simulation. Borehole logs data from 22 wells were used to help define the limits of the various lithostratigraphic units at the different locations in the study area. These data too served as inputs during model conceptualisation. Groundwater levels obtained from 48 hand-dug wells and boreholes together with the corresponding surface elevations of data points were used to calculate the hydraulic heads. These parameters are useful during calibration of numerical model.

The primary data included water samples collected from open wells, boreholes and surface water sources. These data were analysed in the laboratory for chloride and stable isotopes of oxygen and hydrogen (^{18}O and ^{2}H). The isotope data assisted in the determination of the contribution of recent rainwater to groundwater recharge in the study area (Yidana et al., 2014). Isotope analysis of water samples was carried out in the Isotope laboratory of the Department of Earth Science, University of Ghana, using the Picarro L2120-*i* Isotopic Water Analyzer following standard procedures as prescribed in the manual (Picarro Inc, 2012). The instrument has a precision of < 0.05‰ and < 0.3‰ for $\delta^{18}O$ and δD respectively. Results of the analysis were reported in terms of the isotopic ratios of ^{18}O and ^{16}O, and ^{2}H and ^{1}H, relative to the Vienna Standard Mean Ocean Water (VSMOW) (thus delta values, δ) in per mil (‰) as defined by the International Atomic Energy Agency. The data was normalised and reported in the delta notation according to equations (1) and (2) (Coplen, 1994). Chloride data on the other hand was used to estimate groundwater recharge based on the chloride mass balance (CMB) technique based on equation (3).

$$\delta^{18}O = \left(\frac{\left(\frac{^{18}O}{^{16}O}\right)_{sample}}{\left(\frac{^{18}O}{^{16}O}\right)_{VSMOW}} - 1 \right) \times 1000 \quad (1)$$

$$\delta^{2}H = \left(\frac{\left(\frac{^{2}H}{^{1}H}\right)_{sample}}{\left(\frac{^{2}H}{^{1}H}\right)_{VSMOW}} - 1 \right) \times 1000 \quad (2)$$

$$R = \frac{Cl(p)}{Cl(gw)} \times P \quad (3)$$

where R, Cl(p), Cl(gw) and P are respectively recharge rate, amount of chloride in precipitation, amount of chloride in groundwater and average annual precipitation. These datasets were carefully studied and compared with the known geology and hydrogeology of the study area to ensure coherency and precision, and processed into usable formats for adequate conceptualisation of the domain. The conceptual model was subsequently converted into a numerical model for steady state simulation.

3.2. Groundwater flow modelling

3.2.1. Conceptualisation of model domain

Conceptualisation of the domain is prerequisite to the construction of any numerical model. Model conceptualisation aids the determination of the fundamental processes in numerical groundwater flow modelling and simplifies the field problems and associated field data such that the system can be readily analysed (Kyei-Baffour et al., 2013). Based on the collated historical data (lithological logs and groundwater levels data) and results of hydrochemical analysis, together with known geology of the area, the hydrogeological framework of the study area was conceptualised using the Groundwater Modelling System, GMS 10.3 (Aquaveo, 2018). Defining the geological framework of the domain being modelled is an important step to conceptual modelling. This included the thickness, lithology, structures, confining units and continuity. The geological framework was established using borehole logs,

geological maps, digital elevation model (DEM) and field mapping. Borehole lithological logs were properly defined, and the various lithologies encountered at various depths in each borehole formed the basis for lithostratigraphic modelling. GMS lithostratigraphic modelling is based on a robust Inverse Distance Weighting (IDW) interpolation technique which uses the top and bottom elevation of each lithology encountered in the boreholes to define the final model thickness and lithological variations along the domain by interpolation to fill cross-sections between holes. The domain was conceptualised as a single layer with spatial variability in thickness as a result of the partial homogeneity in the lithology and hydraulic properties, coupled with limited drill log data. The lower limit of the aquifer or the fresh granitic layer at the bottom of the aquifer was conceptualised a no-flow boundary or confining layer to reflect the low hydraulic conductivities of the impervious rock, while the upper limit of the domain was conceptualised as unconfining to represent the predominant conditions of direct vertical recharge from precipitation as reported in previous similar studies within the Voltaian (Yidana et al., 2015, 2011, 2008).

The flow of groundwater is also controlled by the surface topography and configurations of the groundwater table, as such, these were analysed and factored in as part of the conceptualisation process. Another vital aspect of model conceptualisation is to define the boundary conditions of the domain. Defining these conditions shows how the boundaries of the model domain interact with the immediate environment; as to whether there is flow in and out of the model domain or not, and the extent of such an interaction. Groundwater head configuration in the study area was found to be almost an exact replica of the topography (Fig. 3a and b); whereby high hydraulic heads are observed in high elevation areas and low hydraulic heads observed in low elevation areas.

Based on field survey coupled with DEM (Fig. 3c), elevation data and groundwater head distribution in the area (Fig. 3b), the vertical boundaries of the model were defined. The existence of hills at the northern and western parts of the area suggests a possible physical boundary which could serve as a groundwater divide, therefore preventing flow across the boundary. Fig. 3b also shows that, the water table contours are perpendicular to the boundary. This is in line with the general hydrogeological knowledge of flow orthogonality, whereby flow of groundwater is usually perpendicular to the water table surface. Based on these observations, no flow boundaries have been assigned to these portions of the entire boundary. Other parts of the boundary were defined as flow-dependent; indicating that the extent of interaction between the model boundary and its immediate environment, in terms of groundwater flow is mainly dependent on the hydraulic gradient and properties of the geologic material at that point. These boundary conditions were adequately digitised and represented in GMS based on MODFLOW.

The study area is also bounded by several rivers and tributaries during the rainy season but in the dry season, most of the tributaries dry off leaving only portions of the Red and White Volta rivers flowing through the eastern and southern portions of the boundary of the district. The White Volta river meanders in and out of the district till it flows down towards the south-western part of the district. The river network was adequately digitised and incorporated into the model, and river conductance and stage and bed elevations assigned accordingly (Fig. 3d). The domain was partitioned for recharge and hydraulic

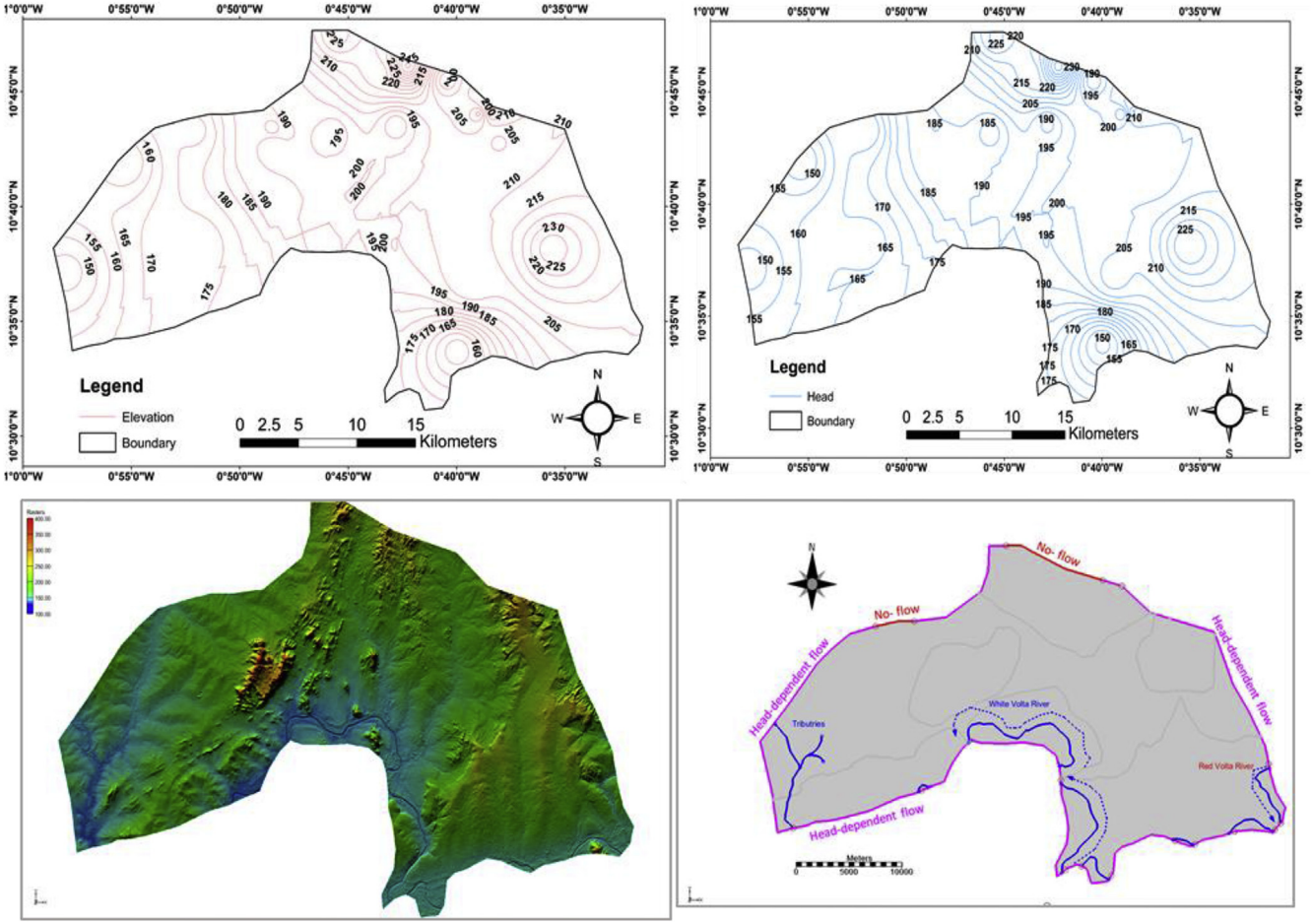

Fig. 3. Conceptualisation of the study area: (a) elevation contours (msl), (b) hydraulic head distribution, (c) digital elevation model and (d) conceptualisation of domain boundary conditions.

conductivity coverages. Hydraulic conductivity values were assigned based on estimates from pumping test, the geology of the zone and guided by similar works done within the Voltaian (Darko, 2015; Obuobie et al., 2012; Yidana et al., 2014). Assigned values ranged between 0.001 m/day and 65 m/day, whilst maintaining a vertical anisotropy of 3 m/day. As a result of the sparse vegetation and topographic variations, groundwater recharge from precipitation in the district is expected to be highly variable, hence the domain was divided into nine (9) main recharge zones and values assigned based on geology, precipitation data, topography, pseudo-confining conditions, isotopic signatures at each zone and recharge estimates by CMB method. Assigned recharge ranged between 2% and 5% of the average annual precipitation of 980 mm/year (5.2×10^{-5} m/day and 1.3×10^{-4} m/day) as reported by previous researches within the Voltaian (Darko, 2015; Obuobie et al., 2012; Yidana et al., 2014).

Characterisation of the groundwater flow system is essential to comprehending its movement through the district. Measured hydraulic heads were used to define likely groundwater flow directions, hydraulic gradient, recharge and discharge zones. Hydrochemical analysis of groundwater also provided qualitative insight into the flow geometry of groundwater in the district. Also, hydraulic heads for the wells were incorporated in the conceptual model, as an observation head coverage. The top and bottom elevations of the wells were imported as 2D scatter points and interpolated to define the model thickness. Forty-eight (48) wells were used for the model calibration, details of which are shown in Table 1.

3.2.2. Choice of code, numerical simulation and model calibration

Myriad numerical codes are available in the literature that are used for the simulation of regional and local groundwater flow systems as also asserted by Yidana and Chegbeleh (2013). However, the modular finite difference code, MODFLOW (Harbaugh et al., 2017), within the Groundwater Modelling System (GMS) version 10.3 (Aquaveo, 2018) was chosen to simulate the groundwater flow system in the study area, due to its demonstrated application and reliability in previous studies. It has been very well tested and used successfully in many modelling situations (Yidana et al., 2013).

The model consisted of 6569 active uniform cells from a 120 × 100 row and column grid discretised over the domain. The conceptual model was then converted into a numerical 3D modular finite difference model based on MODFLOW (Harbaugh et al., 2017), in GMS, so as to enhance simulation of the initial conditions and allow for model predictions.

Prior to using a model for prediction, the model must be fully calibrated to match field-measured parameters of the system under consideration. Model calibration refers to varying model input parameters within a specified range guided by literature and other field measurements till the model computed output matches the observed field conditions with an acceptable margin of error. Models can either be calibrated under steady state or transient conditions (equations (4) and (5)). Steady state model simulations eliminate the time terms in the governing equations (equation (4)) and provide a snapshot of the hydraulic conditions in a stable aquifer system. The current model was calibrated under steady state conditions (convertible) to give a snapshot of the hydraulic conditions of the domain in an equilibrium state. Calibrated steady state parameters are usually used as initial conditions for transient calibrations for better representation of the groundwater system.

$$\frac{\partial}{\partial x}\left(K_{xx}\frac{\partial h}{\partial x}\right) + \frac{\partial}{\partial y}\left(K_{yy}\frac{\partial h}{\partial y}\right) + \frac{\partial}{\partial z}\left(K_{zz}\frac{\partial h}{\partial z}\right) - W = s_s\frac{\partial h}{\partial t} \quad (4)$$

$$\frac{\partial}{\partial x}\left(K_{xx}\frac{\partial h}{\partial x}\right) + \frac{\partial}{\partial y}\left(K_{yy}\frac{\partial h}{\partial y}\right) + \frac{\partial}{\partial z}\left(K_{zz}\frac{\partial h}{\partial z}\right) = 0 \quad (5)$$

where Kxx, Kyy, and Kzz are respectively, the hydraulic conductivities (LT^{-1}) which can vary in the x, y and z directions, whereas h, W, S_S and t are the hydraulic head (L), sources/sinks (L^3T^{-1}), specific storage and time (T) respectively.

The model was calibrated to hydraulic head data collected in the study area, by altering assigned hydraulic parameter such as hydraulic conductivity values and recharge. The calibration was a combination of both manual and automated calibration. Manual calibration involved "trial and error", in which small changes were made to input parameters, mapped to MODFLOW and ran each time. Though this type of calibration is time consuming, it allows the modeller to deduce understanding of the system in the calibration process, as well as providing hint to the modeller on the hydraulic parameters that most impact the model. The automated calibration on the other hand was carried out using Parameter Estimation (PEST). In this method of calibration, the value of the parameter within each zone is interpolated

Table 1
Summary of wells used for model calibration.

ID	Easting	Northing	Elevation (m)	SWL (m)	Head (m)	ID	Easting	Northing	Elevation (m)	SWL (m)	Head (m)
CWS01	758786.68	1185239.68	204	2	202	CWS25	734496.37	1181622.62	182	2	180
CWS02	758154.58	1187746.88	223	8	215	CWS26	733806.16	1172821.53	178	2	176
CWS03	757667.75	1188440.32	209	3	206	CWS27	735328.02	1172161.99	151	1	150
CWS04	733173.82	1186048.50	173	13	160	CWS28	733022.17	1176740.97	169	2	167
CWS05	745263.59	1193769.54	232	6	226	CWS29	738289.13	1178753.84	168	3	165
CWS06	739737.32	1186315.90	187	3	184	CWS30	736315.03	1180639.46	192	3	189
CWS07	741098.79	1188726.75	199	5	194	CWS31	736712.18	1180795.91	191	2	189
CWS08	740550.37	1187383.95	196	4	192	CWS32	740016.43	1185537.19	190	3	187
CWS09	760121.25	1182483.35	210	7	203	CWS33	740234.40	1185661.69	191	1	190
CWS10	751080.07	1191378.21	261	9	252	CWS34	744196.88	1185416.63	181	2	179
CWS11	754371.64	1190185.77	191	5	186	CWS35	744258.17	1185349.45	181	2	179
CWS12	748491.74	1190728.18	222	5	217	CWS36	749120.95	1186291.83	185	5	180
CWS13	750109.34	1186557.36	191	3	188	CWS37	751609.83	1186387.19	189	1	188
CWS14	733379.15	1176910.62	171	9	162	CWS38	751666.91	1186071.01	185	2	183
CWS15	744752.49	1185842.99	191	9	182	CWS39	733843.74	1185432.30	171	7	164
CWS16	755410.50	1168504.21	157	8	149	CWS40	756294.66	1185933.78	189	2	187
CWS17	757018.06	1187538.98	194	3	191	CWS41	757834.26	1184958.79	191	2	189
CWS18	739768.89	1184955.13	199	10	190	CWS42	761142.72	1175393.32	189	4	185
CWS19	763339.95	1176753.64	233	3	230	CWS43	760671.37	1180929.06	174	3	171
CWS20	756462.93	1174155.78	210	3	208	CWS44	762978.40	1178281.72	142	5	137
CWS21	727282.62	1183463.46	155	9	146	CWS45	757081.07	1167994.17	138	5	133
CWS22	722416.86	1174579.98	148	8	140	CWS46	755848.46	1175393.01	143	5	139
CWS23	734282.14	1181390.62	170	4	166	CWS47	732858.22	1185536.12	179	7	172
CWS24	734121.71	1181730.67	176	7	169	CWS48	733754.92	1181580.60	177	2	175

from values assigned to the pilot points or polygons in it, whilst the inverse model estimates values at each point by readjusting the pilot point/polygon values to minimise the objective function. Optimal balance between the observed and computed heads were determine by comparing error statistics, such as Root Mean Square error (RMS), Mean Absolute Error (MAE) and Mean Error (ME) (Kyei-Baffour et al., 2013).

3.2.3. Sensitivity analysis

Sensitivity analysis is the assessment of model input parameters to measure model stability and their effect on model outputs (Anderson and Woessner, 1992). Sensitivity analysis also is inherently part of model calibration, hence highly sensitive parameters are the most important parameters that cause the model to match observed values. A model that is highly sensitive to a particular parameter is considered unstable and therefore, not suitable for predictions. In this study, sensitivity analysis was carried out to identify model parameters and boundary conditions that influenced the model results. This was automatically done through PEST and histograms were generated at the end of the calibration to indicate parameter sensitivities. The model was well calibrated against the recharge rates and hydraulic conductivity.

3.2.4. Scenario analysis

Although a transient model is best fit for scenario analysis, since it can sufficiently depict fluctuations in groundwater storage. However, in the absence of transient data, the steady state model was used in a limited manner to simulate various scenarios of stresses on the underlying aquifer. Initial flow rates assigned to the wells were estimated based on the daily water consumption of 70 L per capita, applied to the total population size of 81,194 people in the district (Talensi District Assembly, 2014). A total of 5684 m^3/day abstraction rate was distributed among the twenty-two (22) abstraction wells across the district which led to the various abstraction rates assigned per well. It is noteworthy that the total abstraction wells or groundwater outlets in the district far exceed twenty-two (22), and this number was only used for purposes of the scenario analysis in this study.

Abstraction rates were increased by 10%, 20%, 50%, 100%, 200% and 500% whilst maintaining recharge at the calibrated rates in the first scenario, to simulate the impacts of population growth, industrialisation and urbanisation and the corresponding increasing demands on groundwater. In the second scenario, the recharge was consciously reduced by 10%, 20%, 40% and 60% whilst abstraction rates were increased at 10%, 20%, 50%, 100%, and 150%. This was also to simulate the possible impacts of climate change which might lead to reduced recharge rates in the wake of increased water demands.

4. Results and discussion

4.1. Lithostratigraphy and aquifer zone

From the twenty-two (22) borehole lithological logs reviewed, a stratigraphic model of the terrain was developed. The 3-dimensional (3D) geological model (Fig. 4) suggests that, the domain is characterised mainly by granite of various degrees of weathering with patches of sandy clay and lateritic materials in the southwestern and northern portions respectively. Weathered quartzite, sandstones and gneisses of variable spatial thickness and extent underlie the weathered granite in the northern and southern portions of the district. Within the limits of the boreholes used, the model suggests the entire district is underlain by fresh granite of variable thickness ranging between 5 and 20 m, therefore imposing confining conditions at the bottom. The variably weathered materials overlying the fresh granitic rocks at the bottom do not suggest any constraining conditions to vertical recharge and hence is indicative of unconfining conditions at the top of the aquifer. However, the degree of vertical recharge is controlled mainly by the hydraulic conductivity and permeability of the geologic materials. Generally, the aquifer zone appears to be within the weathered granite, sandstone and gneiss.

4.2. Hydraulic potential field

The calibrated steady state model showing the hydraulic head distribution and flow geometry of groundwater across the district is presented in Fig. 5. The model shows a reasonably good match between the field measured (observed) hydraulic heads and the model computed heads of the 48 boreholes used for calibration (Fig. 6), with a root mean squared residual (head) of 0.90. This suggests that, the model-estimated parameters are reasonably representative of the hydrogeologic conditions of the modelled domain within the limits of the data used, and therefore the model is deemed fit for fairly reliable prediction of various scenarios of abstraction and other stresses on the aquifer system. The highest hydraulic heads are in the eastern and south-eastern sections of the study area. There is a general northeast-southwest flow pattern with a few local flow systems, which cannot be clearly defined. Yidana et al. (2010, 2013) observed similar flow patterns in the crystalline basement aquifers of the Birimian in southeastern and southwestern Ghana.

The general flow pattern appears to follow the topographic configurations of the district, which is in keeping with the fact that the water table is usually a subdued replica of the surface topography; where topographic highs and lows are respectively identified as recharge and discharge zones. The hydraulic heads in the area generally range from 80 m to 284 m (Fig. 5), and suggests good fortunes for potential groundwater development for irrigation and industrial activities in the district which could go a long way to support the livelihood of the indigents, especially in the long dry season.

4.3. Hydraulic conductivity field

The horizontal hydraulic conductivity (K) field in this study was estimated using pilot points in automated parameter estimation (Hill et al., 2000) method. The resultant model-calibrated hydraulic conductivity field (Fig. 7) suggests a highly heterogeneous system, with values varying between 0.001 m/d and 58.396 m/d. The K values appear not to vary according to the geological formations in the district, however the highest and lowest values occur within the crystalline basement rocks of the Birimian, which suggests good fortunes in terms of groundwater delivery and potential groundwater development. This ties in well with the assertion that aquifers of the Birimian Supergroup are among the most prolific in terms of groundwater delivery in Ghana (Banoeng-Yakubo et al., 2010). However, the largest portion of the district has hydraulic conductivity values which fall within the range of 0.001–6.5 m/d, although there are patches of high hydraulic conductivity values in the central, western and south-eastern sections of the district, a phenomenon Yidana et al. (2015) attribute to deep seated fracturing/weathering of the rocks. The groundwater flow pattern seems not to have any trend with the hydraulic conductivity field, which also suggests that horizontal hydraulic conductivity varies significantly from vertical hydraulic conductivity which controls vertical groundwater recharges and that baseflows may be the main source of groundwater recharge in the domain (Yidana et al., 2013).

4.4. Model estimated groundwater recharge

Fig. 8 presents the spatial distribution of model estimated vertical groundwater recharge for the Talensi District. The recharge values range between 4.23×10^{-3} mm/day and 8.97×10^{-2} mm/day which translates into 0.16% and 3.34% of the annual precipitation in the district. These values are within the ranges reported by Attandoh et al. (2013) and Yidana et al. (2010) for aquifers in the Voltaian and Birimian in northern and southeastern Ghana. The quantification of groundwater recharge is essential for effective management of the resource, because it forms the basis for allocating groundwater

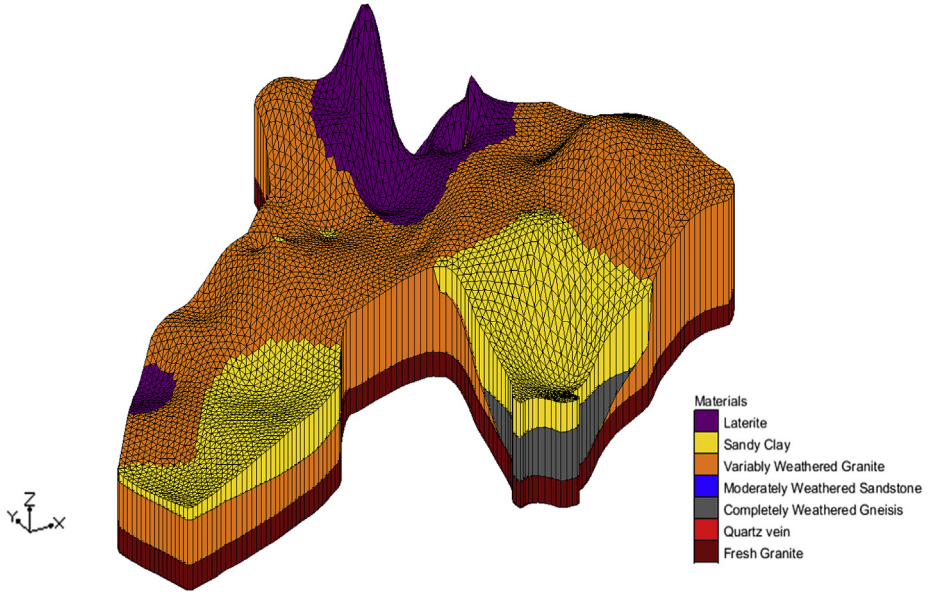

Fig. 4. 3D geological model developed from the borehole logs.

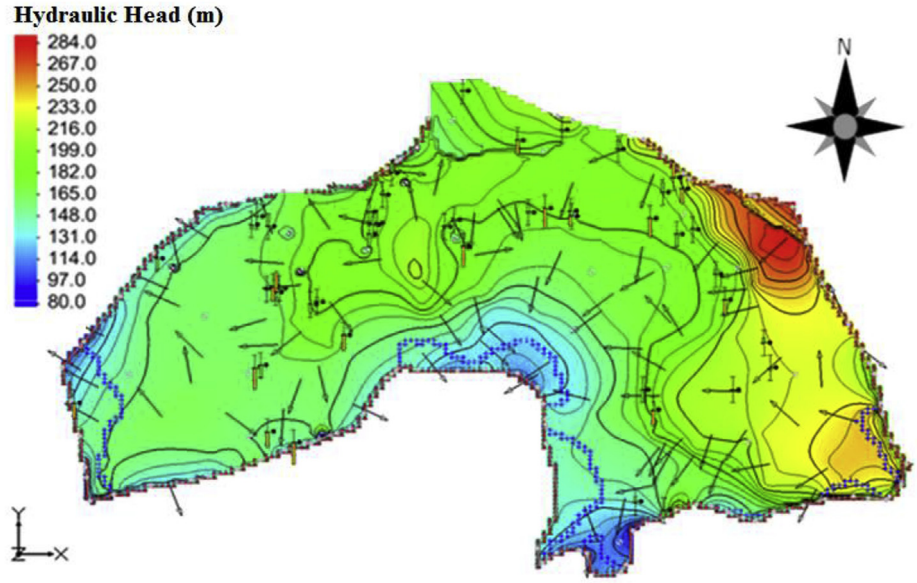

Fig. 5. Calibrated hydraulic head distribution.

abstraction rates. Vertical groundwater recharge is however determined to a large extent by the permeability and hydraulic conductivity of the rock matrix through which the water flows. The hydraulic conductivity field as established in this study is not homogeneously distributed in the rock mass, and because the permeability of fractured systems is highly sensitive to the fracture aperture and degree of fracture connectivity, it is very difficult to predict groundwater recharge in crystalline rocks, especially using models. However, a properly constructed and calibrated model can be used to sufficiently assist in understanding the regional hydrogeology of an aquifer (Ophori, 1999).

4.5. Recharge estimation using chloride mass balance

The estimated recharge using CMB method ranged between 0.55% and 21.73% with an average of 2.07% of the average annual precipitation in the district. These results are in tandem with recharge estimates by Obuobie et al. (2012) within the Upper East Region, which ranged between 3% and 19% of the average annual precipitation of 990 mm/year using the CMB approach.

Fig. 9 presents the spatial prediction map of groundwater using the point estimates of recharge from the CMB technique based on inverse distance weighting (IDW) technique (RMSR = 0.26). Prior to the spatial interpolation, the recharge rates were log transformed to approximate normality, for optimal statistical analysis since the dataset is stationary already. The prediction map (Fig. 9) shows a highly variable recharge rate with no well-defined pattern. The high variability in recharge is attributable to the diverse prevailing soil and topographic conditions which characterise the district, which might result in different infiltration rates across the district. Notwithstanding the heterogeneity, high recharge rates appear to occur around Tula and Bingo, in the north-east portions of the district whilst the lowest values occur around Pwalugu and Shia in the northern and eastern sections of the district. High elevation areas are associated with high rainfall events as a result of the interaction of topography with the atmosphere (Subarna et al., 2014). As such, based on the CMB assumptions, chloride concentrations decrease with elevation as a result of high precipitation, low

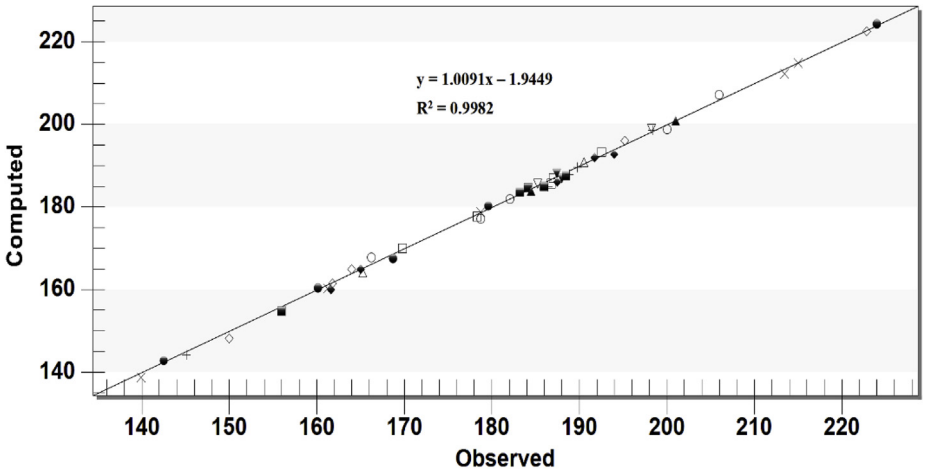

Fig. 6. Calibration plot showing observed versus computed water levels.

temperatures and associated low evaporation rates. Although the elevations of the district are relatively flat and do not vary much (400 m–100 m), the district still exhibits direct positive relationship with precipitation (or recharge) and inverse relation with chloride concentration in groundwater with elevation (Fig. 10), which suggest chloride in the district is of meteoric origin (Houston, 2007).

4.6. Groundwater recharge characterisation

4.6.1. Isotope analysis

Stable isotope content of rainwater, rivers, dams and groundwater are presented with a box and whisker plots shown in Fig. 11. Rainwater and river water samples seem to show the highest ranges and variations in δ^2H and $\delta^{18}O$ among the various water sources in the district (Fig. 11a). δ^2H and $\delta^{18}O$ values for rainwater range from −79.18 to −12.19, and −10.15 to −1.75, with standard deviations of 17.34 and 2.19 respectively. River water samples on the other hand have δ^2H and $\delta^{18}O$ ranges from −20.29 to 4.09, and −3.5 to 1.2, with standard deviations of 10.23 and 2.06 respectively (Table 2). However, isotopic contents of δ^2H and $\delta^{18}O$ for the river water samples are generally higher than those displayed by the rainwater, indicating that water from the rivers is more enriched in stable isotopes than rainwater within the district; the high standard deviations of rivers reflect the widespread variety of environmental settings prevailing in the area. Rivers are usually exposed to impact of several weather conditions such as high temperatures and evaporation rates as the water transits from one location to another, hence the enrichment and high variability in the isotopic composition (Addai et al., 2016). Besides the contribution of the Gulf of Guinea to precipitation in the region, re-evaporated water from surface water bodies such as rivers and streams in the region play a role in the isotopic signatures of rainwater in the area, and thus reflect the wide range of sources and conditions. Low atmospheric humidity is also known to cause evaporation of rain drops, leading to isotope enrichment of rainwater (Addai et al., 2016).

Furthermore, isotopic signatures of δ^2H and $\delta^{18}O$ in groundwater and dam water in the district appear to display small ranges and deviations relative to rainwater and river water. The exhibited isotopic contents of δ^2H and $\delta^{18}O$ are in the range of −27.85‰ to −9.33‰, and −2.43‰–1.51‰ respectively for groundwater, and dam water in the range of −2.55‰–9.96‰ and 1.92‰–5.12‰ respectively, whereas standard deviations for δ^2H and $\delta^{18}O$ in groundwater and dam water are respectively 3.25‰ and 0.66‰, and 4.83‰ and 1.06‰ (Table 2). The apparent relative homogeneity of the groundwater data suggests that similar factors such as the sources of recharge might be

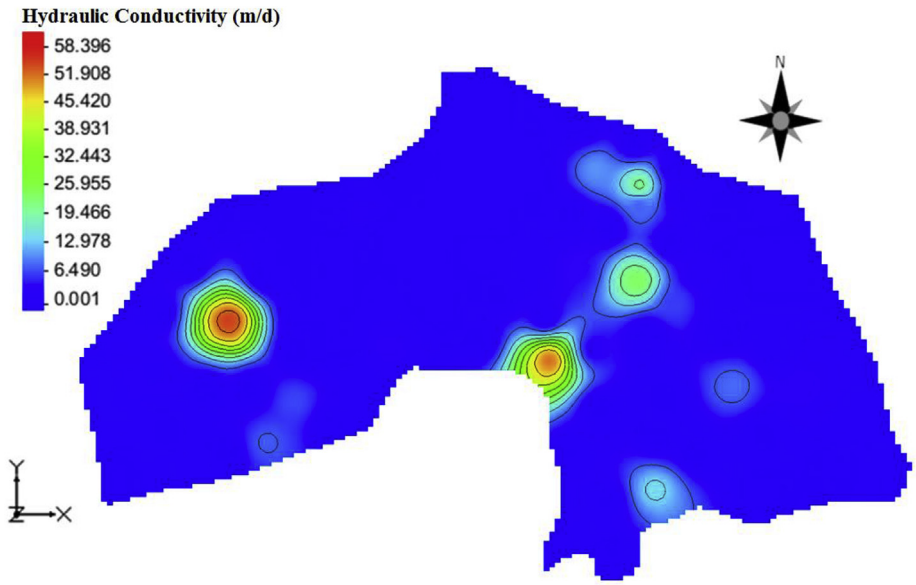

Fig. 7. Calibrated hydraulic conductivity field showing the variations of the horizontal hydraulic conductivity distribution in the district.

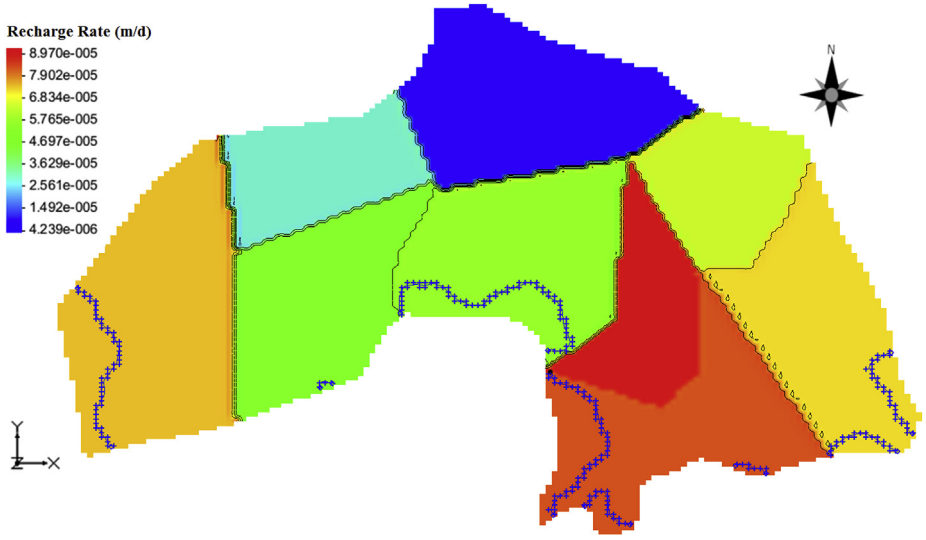

Fig. 8. Model estimated vertical groundwater recharge rate.

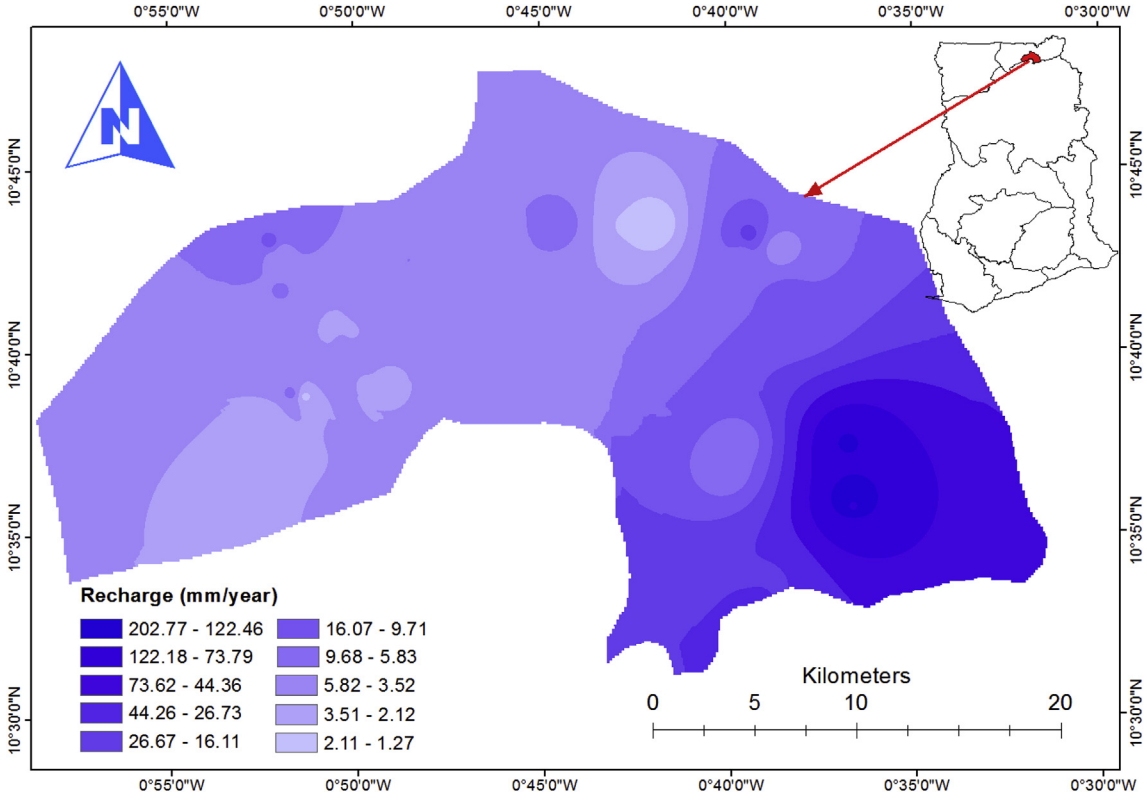

Fig. 9. Chloride mass balance estimates of recharge in Talensi District.

similar in space and/or in time, hence influencing the isotopic signatures as exhibited by groundwater in the area.

The outliers in the groundwater isotopes (Fig. 11) are attributable to evaporative enrichment of groundwater in areas where groundwater levels are close to the surface conditions, hence affected by evaporation under high ambient temperatures and low relative humidity; conditions common on the surface. This is particularly true for the long dry season period in the area which was the time of sampling for this study. This is consistent with the assertion by Addai et al. (2016), that evaporation is an active process in groundwater at 3 m below the ground surface in some portions of the White Volta basin in northern Ghana.

Deuterium-excess (d-excess) has also been computed (based on equation (6)) for the various water sources in the district and presented below (Table 2 and Fig. 12). Deuterium-excess aids in the determination of vapour sources in a region which eventually forms precipitation that recharges groundwater or surface water bodies. Rainwater and water from rivers show the highest variations and ranges in d-excess values, with mean values of 9.85‰ and 4.31‰ respectively (Fig. 12). The d-excess value defined by the GMWL (Craig, 1961) is 10‰ (according to equation (6)), hence d-excess values below this value suggest a relative evaporative enrichment.

$$\text{D-excess} = \delta^{2}\text{H‰} - 8\delta^{18}\text{O‰} \quad (6)$$

The mean values of d-excess for all the water sources sampled are

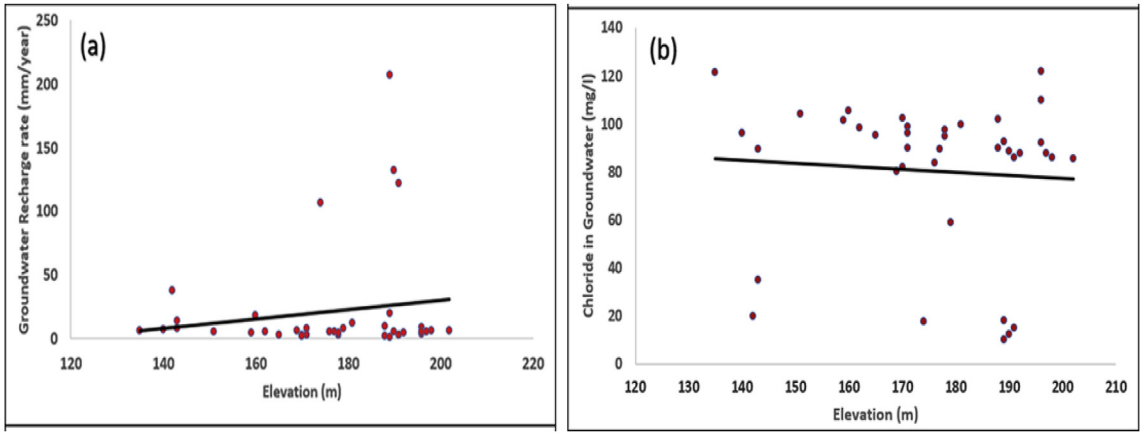

Fig. 10. Relationship between (a) groundwater recharge estimated through CMB versus elevation (m.a.s.l) and (b) chloride concentration in groundwater versus elevation (m.a.s.l) in the study area.

below 10‰ (Table 3), suggesting relative evaporative enrichment in rainwater, rivers, dams and groundwater in the district as compared to that of the GMWL. Dam water shows the lowest d-excess values followed by groundwater, river water and rainwater respectively. Addai et al. (2016) attribute low d-excess values in rainwater to kinetic fractionation, following evaporation of rain drops which eventually results in enrichments in heavier isotopes in rainwater. The relative evaporative enrichment of rainwater is characteristic of the district which is characterised by low annual rainfall, low humidity, high temperatures reaching 45 °C and persistent high wind speeds which result in the evaporation of rain droplets in the course of the event.

4.7. Relative evaporation lines for rainwater, groundwater and surface water

To understand the evaporative enrichment or otherwise of the different sources of water sampled in the district, a comparative analysis is carried out by comparing linear plots of precipitation, surface water sources (rivers and dams), groundwater and the GMWL, and establishing the relationships that exist among them. Craig (1961) established a linear relationship between δ^2H and $\delta^{18}O$ in precipitation defined by the GMWL (equation (7)). The stable isotopes values of groundwater, surface water sources in the district and rainwater samples collected from Navrongo Meteorological Station have been plotted on a binary plot (Fig. 13). The linear plot of δ^2H versus $\delta^{18}O$ in rainwater with a regression line was used to derive the Local Meteoric Water Line (LMWL) for the district (equation (8)) to aid discussions of the results.

$$\delta^2H = 8\delta^{18}O + 10 \quad (7)$$

$$\delta^2H = 7.3\ \delta^{18}O + 7.8 \quad (8)$$

The LMWL presents a gradient and intercept of 7.3 and 7.8 respective, both of which are lower than that displayed by the GMWL, hence corroborating that rainwater is indeed relatively enriched in stable water isotopes compared to the GMWL. This enrichment in isotopic composition is attributable to evaporation as a result of climatic conditions in the district such as the low relative humidity, high temperature and windy conditions in the dry season, which Gonfiantini (1986) suggest could lower the slope of the LMWL. However not all the rainwater samples plot below the GMWL (Fig. 13), which indicates that the isotopic composition of precipitation in the district is highly variable and do not deviate significantly from the GMWL.

All other water sources such as the rivers, dams and groundwater plot below the GMWL, with different levels of departure from the regression lines for the GMWL and LMWL. These departures are attributable to relative evaporative enrichment in the isotopic composition of these other water sources in the district, since the study area in characterised by high temperature and low relative humidity which rarely exceed 80% (Addai et al., 2016; Afrifa et al., 2017).

The regression line for the rivers in the district (equation (9)), unlike the precipitation present a very shallow gradient with a corresponding negative intercept; which suggest rivers in the district are highly

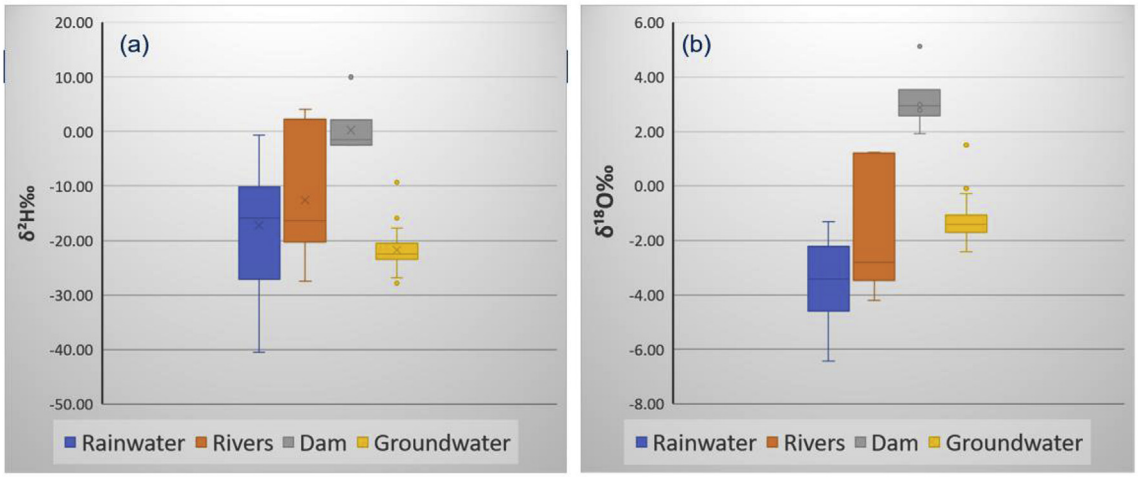

Fig. 11. Box plots for δ^2H‰ (a) and $\delta^{18}O$‰ (b) from various water sources in the district.

Table 2
Statistical summary of isotope data.

	$\delta^{18}O$‰ (Rain)	$\delta^{18}O$‰ (Rivers)	$\delta^{18}O$‰ (Dam)	$\delta^{18}O$‰ (GW)	$\delta^{2}H$‰ (Rain)	$\delta^{2}H$‰ (Rivers)	$\delta^{2}H$‰ (Dam)	$\delta^{2}H$‰ (GW)
Mean	−8.278	−1.734	3.124	−1.308	−56.376	−11.464	.226	−21.759
Median	−8.913	−2.820	2.949	−1.406	−57.566	−16.410	−1.499	−22.452
Mode	−10.150	−3.500	1.924	−2.427	−79.180	−20.290	−2.549	−27.856
Std. Deviation	2.198	2.057	1.061	.664	17.335	10.233	4.837	3.255
Variance	4.830	4.229	1.126	.441	300.517	104.710	23.395	10.593
Range	8.41	4.7	3.200	3.934	66.993	24.38	12.509	18.530
Minimum	−10.15	−3.5	1.924	−2.427	−79.180	−20.29	−2.549	−27.856
Maximum	−1.75	1.2	5.124	1.507	−12.187	4.09	9.960	−9.326

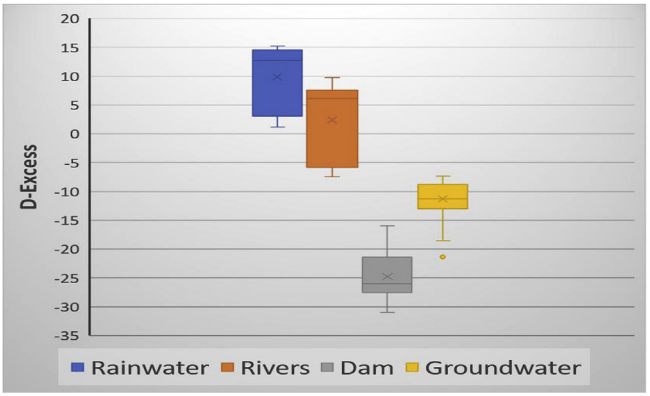

Fig. 12. Deuterium-excess distribution in the various water sources in the district.

Table 3
Statistical summary of deuterium-excess for various water sources.

D-excess	Groundwater	Rain	Rivers	Dam
Mean	−11.29	9.85	4.31	−24.77
Minimum	−21.38	1.2	−7.42	−31.03
Maximum	−7.38	15.26	15	−15.94
Range	14	14.06	22.42	15.09
Std. Deviation	2.96	5.63	8.76	5
Skewness	−1.25	−0.66	−0.3	1.05
Std. Error Skewness	0.38	0.64	0.79	0.85
Kurtosis	2.65	−1.43	−1.67	2.3
Std. Error Kurtosis	0.74	1.23	1.59	1.74

affected by evaporative effects. The relatively high evaporation of rivers is quite logical, since these water bodies are exposed to multitude adverse weather conditions such as high temperatures, low relative humidity and high wind speeds for prolonged periods of time thereby allowing substantial amounts of the river water to evaporate.

$$\delta^{2}H = 5.15\delta^{18}O - 2.95 \quad (9)$$

Equation (9) is in tandem with assertions that relative humidity below 100% during precipitation could result in a $\delta^{2}H$–$\delta^{18}O$ plot line gradient that results from precipitation to be 5 ± 2 (Gonfiantini, 1986). The high variation associated with the river water (Table 2) suggest that the river waters traversed and transited different environmental conditions to the various locations where they were sampled. Rivers are also known to be recharged by baseflow, interflow, and contributions from tributaries which represent different water sources (Addai et al., 2016), and hence the high variation and deviation in the isotopic signatures of river waters. Groundwater on the other hand presents an even shallower slope with a negative intercept (−16.2) (equation (10)). This could have resulted from evaporation of precipitation at the time of recharge to groundwater or evaporation on the free surface or raindrops before infiltration into the soil zone (Addai et al., 2016; Afrifa et al., 2017; Pelig-Ba, 2010) or isotopic exchange with aquifer materials such as silicate minerals richer in $\delta^{18}O$ (Domenico and Schwartz, 1990).

$$\delta^{2}H = 4.3\delta^{18}O - 6.2 \quad (10)$$

The regression equation obtained for groundwater by Pelig-Ba (2010) (equation (11))

$$\delta^{2}H = 5.7\delta^{18}O - 7.3 \quad (11)$$

Comparing the regression line obtained by Pelig-Ba (2010) for groundwater in the Northern Region of Ghana; which has almost similar climatic conditions (dry savanna zone) as the current study area, it is clear that groundwater in the study district is more enriched in heavy isotopes. Generally, groundwater is usually depleted in stable water isotopes than surface water sources, due to the exposure of surface water to the weather conditions in a place (potential evaporation), however in this particular study, the groundwater seemed enriched than water from the rivers. This might have resulted from an upstream precipitation event that occurred around the period of sampling, therefore diluting the isotope composition of rivers in the area which resulted in the river waters being less enriched than the groundwater. This assertion is corroborated by the relatively high enrichment of water samples from the dams which are more localised and could not have been affected by this probable upstream precipitation event. The relative depletion of heavier isotopes in the Northern Region from Pelig-Ba (2010) study however is attributable to direct recharge from local precipitation from preferential flow through macro pores to the groundwater with low level of mixing with fresh precipitation (Clark and Fritz, 1997).

Dam water stable isotope data displayed the highest enrichment, with the lowest slope of 3.9 (equation (12)). This is logical owing to the fact that dams generally have large surface areas, hence more of the water is exposed to the direct sunlight, heat and air, as a result, increasing evaporation rate of the water.

$$\delta^{2}H = 3.9\delta^{18}O - 11.9 \quad (12)$$

4.8. Relationship and interaction between various water sources

It is obvious for the various water sources in the district to display common relationships since they most likely derive from the same source–precipitation. However, isotope analysis can be used to understand the nature and extend of these interactions and relationships. During precipitation events, the water normally collects in channels and on the land surface as runoffs and transported into depressions such as dams and rivers or falls directly into these rivers and dams. As such the surface water sources exhibit isotopic composition close to the local precipitation in the area as shown by the plots in the green enclosure (Fig. 14). Some of the surface water (plots in purple and yellow enclosures) plot drift away from the precipitation plots, which indicates the possible evaporations of these water sources. However, some river water and groundwater show some close relationship (purple enclosure) although the river water is suspected to have been diluted by a possible recent precipitation event upstream (Fig. 13). The orange

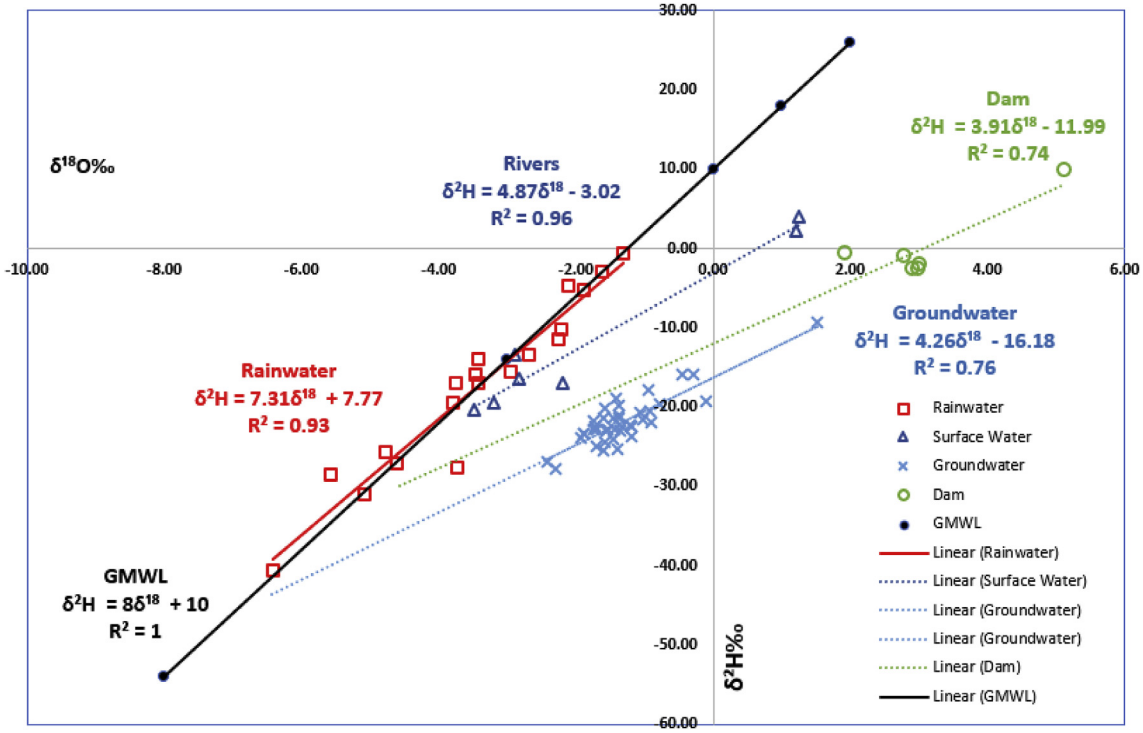

Fig. 13. Biplot of stable isotopes of δ^2H versus $\delta^{18}O$ comparing regression lines of rainwater, rivers, dam water, groundwater and the global meteoric water line.

enclosure also suggests direct recharge of groundwater from precipitation with little mixing, which could occur through cracks and crevices which characterise the Basement Complex (Pelig-Ba, 2010) that underlie the study area. The river water sample which plots close to the groundwater sample in the purple enclosure is a well sampled in Pwalugu, about 0.8 km away from the White Volta river, and therefore suggest a hydraulic connection between the river and groundwater. The degree of this interconnection is however determined by the conductance of the river bed.

4.9. Spatial distribution of stable isotopes in Talensi District

The isotope data of δ^2H and $\delta^{18}O$ in the district appear to be variably distributed and not in a particular direction based on the undefined spatial pattern. This suggest different soil materials with dissimilar porosity ranges overlie the district, as a result precipitation

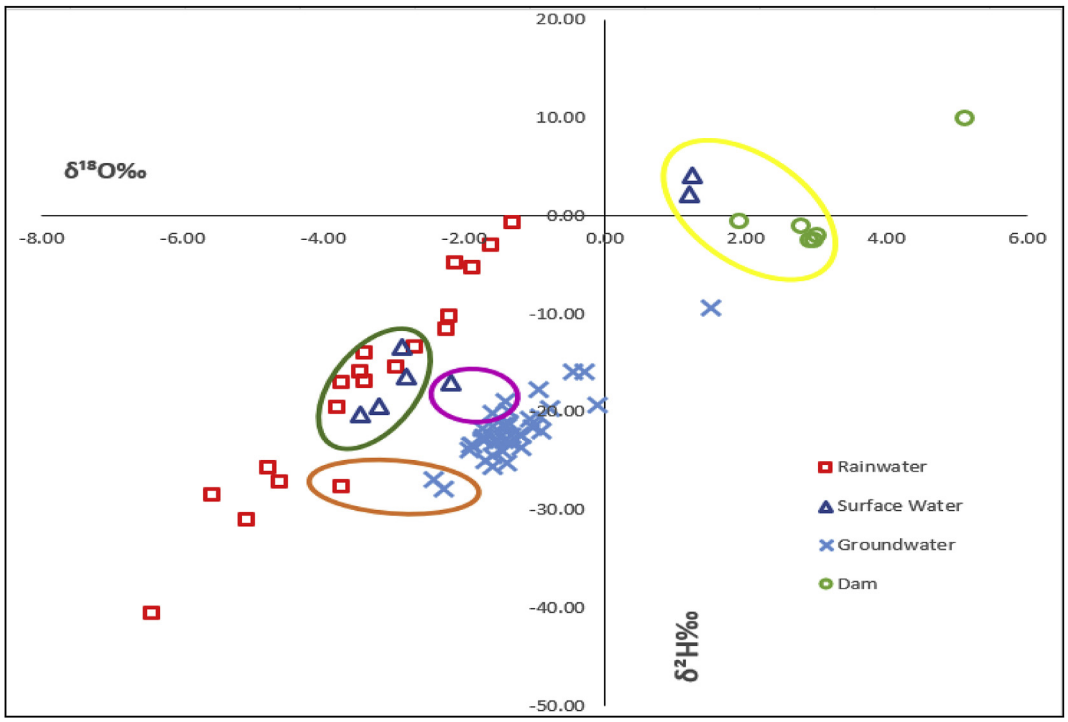

Fig. 14. Relationships between rainwater, surface water sources and groundwater.

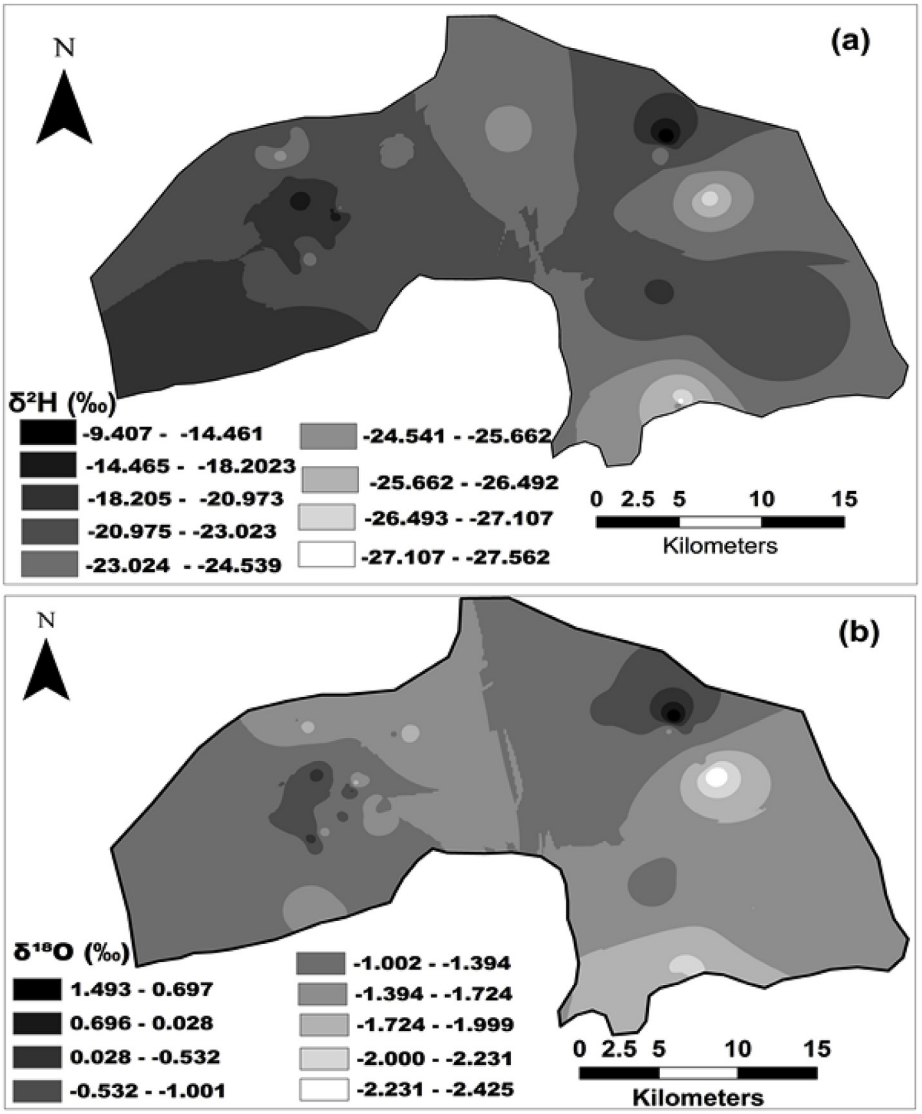

Fig. 15. Spatial prediction maps of the stable isotopes of (a) δ^2H‰ and (b) δ^{18}O‰ of groundwater samples in the study area.

interact diversely in the unsaturated zone before recharging groundwater. However, the ranges and means of isotope data in the geologic units suggest that groundwater in the south-eastern parts of the district, the Voltaian is more depleted in δ^2H and ^{18}O isotopes than the Basement complex (northern and central parts) (Fig. 15). This could be attributable to the relatively high secondary porosity in the Voltaian than the Basement Complex which is characterised by crystalline rocks such as granite and monzonite. This gives rise to preferential flow of precipitation through faults, cracks and crevices in the Voltaian, as result not allowing a high level of mixing of the rainwater prior to recharge of groundwater, hence the high levels of isotopic depletion in the Voltaian. Pelig-Ba (2010) made a similar observation in the Northern Region of Ghana where the underlying geology is similar to that of the current study area. The south-western portions of the study area appear to display enrichment in stable water isotopes, with patches of high values also occurring around the north-eastern portions (Fig. 15). The enrichment around the south-western portion is associated with the Eburnean Plutonic Suite which underlies it. The Eburnean Plutonic Suite are mainly granitoid intrusions of the Basement rocks in the area, and are therefore characterised by very low porosities associated with crystalline rocks. Hence precipitation on this geologic material takes time to finally recharge groundwater, allowing the local precipitation in the soil zone to be exposed to the weather conditions such as the sunlight and evaporation for long periods of time, consequently resulting in enriched isotopic signatures in that portion of the district as a result of the evaporation.

The isotope data suggest that prior to, and in the process of infiltration and final recharge of groundwater, precipitation and water in the soil zone undergo evaporative enrichment such that the water that finally recharges groundwater is rich in heavier isotopes than the local and global meteoric water. This suggest that evaporation significantly affect the quantity of precipitation that recharges groundwater in the district, hence projected rise in temperature as a result of climate variability in the near future may increase evaporation of infiltrating precipitation resulting in reduced groundwater amounts in the study area.

4.10. Scenario analysis

Scenario analysis reveals the various pathways of change to groundwater resources that may arise from certain coherent and calculated assumptions, which ultimately leads to alternative possible future states of the resource. Consequently, providing a dynamic and flexible way of effectively evaluating the possible impacts, dangers, benefits and management prospects arising from a variety of conceivable future conditions. Scenario analysis in this study aimed at

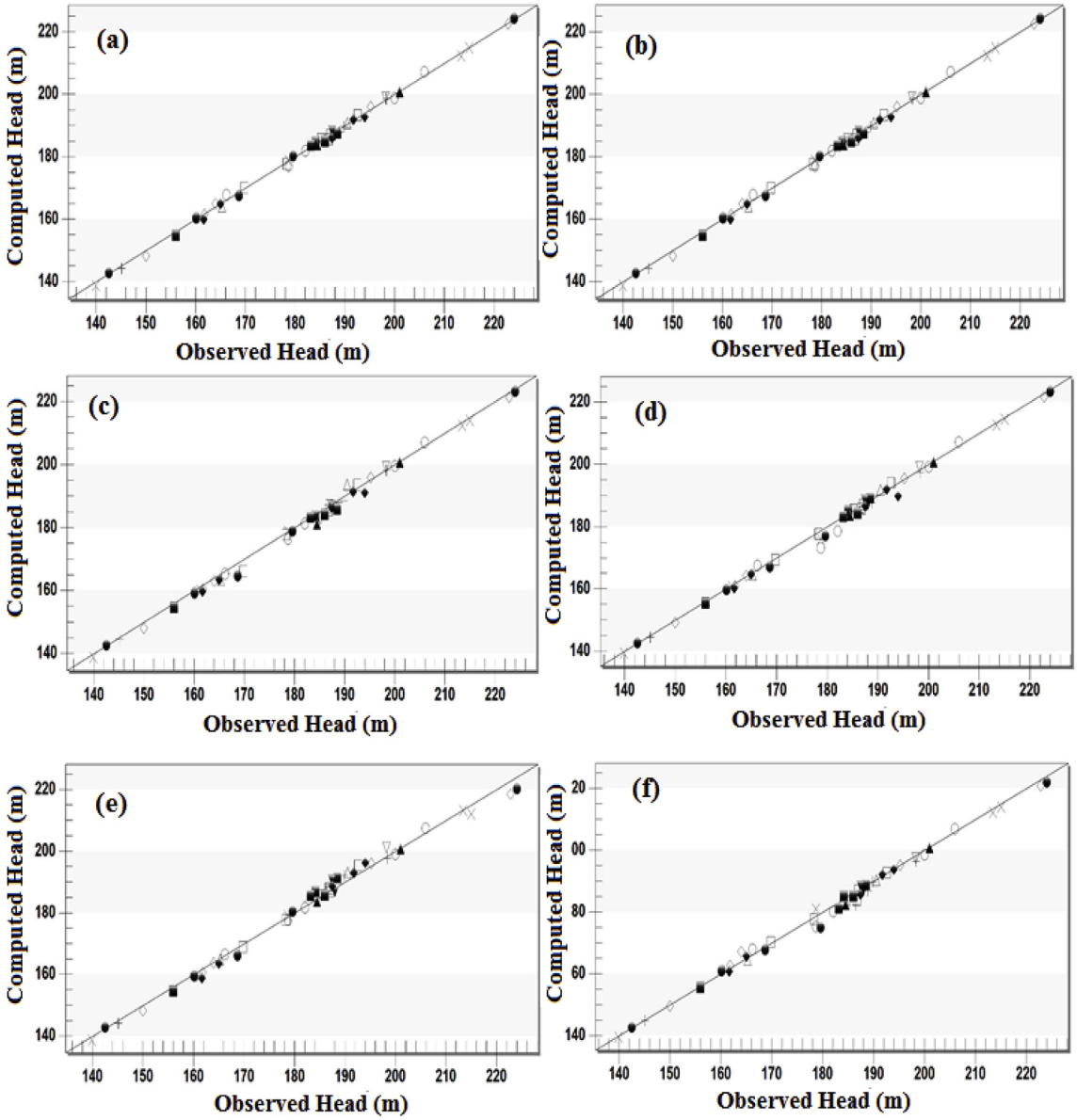

Fig. 16. Observed versus computed hydraulic head after (a) 10%, (b) 20%, (c) 50%, (d) 100%, (e) 200% and (f) 500% increase in abstraction rate from 22 wells.

particularly identifying the sustainable maximum abstraction rates for potential commercial uses from all wells through the underlying aquifer and the possible impacts of recharge reduction resulting from potential climate change impacts. Thus, abstractions rates that would maximise groundwater usage for various purposes without actually negatively impacting on the hydraulic head distribution in the district and groundwater availability for future usage.

The steady state model was used to simulate the first scenario which involved maintaining model-estimated recharge values whilst increasing current abstraction for the wells by 10%, 20%, 50%, 100%, 200%, and 500%, whilst observing the impacts on the hydraulic head. This assumption sought to factor in the impacts of populations growth and the associated increasing water demand on model-estimated hydraulic head distribution in the district, in an instance where basin-wide groundwater recharge is maintained at the present rate.

Th effects of applying the first scenario are presented in Fig. 16 for comparison with Fig. 6. It has been observed that increasing groundwater abstraction through the existing wells by up to 100% do not appear to have any noticeable effects on the groundwater levels under the current recharge rates of 1.54–32.74 mm/year, and that the system could sustain increased abstractions by up to five folds (500%). However, significant changes from calibration and general groundwater flow patterns was evident, with the cones of depression of the abstraction wells widening as abstraction rates exceed 100%. The observation in this scenario implies that the underlying aquifer holds good fortunes for potential groundwater development for large-scale abstractions such as for irrigated agriculture and water demands associated with urbanisation.

But for significant withdrawals beyond 100% of the current abstraction rate, such as for irrigated agriculture, groundwater recharge would have to increase to sustain the fortunes of the aquifer. This is however unlikely since climate variability has been predicted to impact rainfall negatively, leading to reduced groundwater recharge (CSIR-WRI, 2000; EPA, 2008) especially in arid and semi-arid areas such as the current study area. Similarly, the model does not support increasing abstraction rate beyond 500%, as it causes a drastic reduction in the hydraulic heads and changes the flow pattern in the domain. Over abstraction of groundwater from the aquifer without allowing adequate time for the system to replenish through vertical recharge or lateral inflow can lead to depletion of the resource. This could consequently

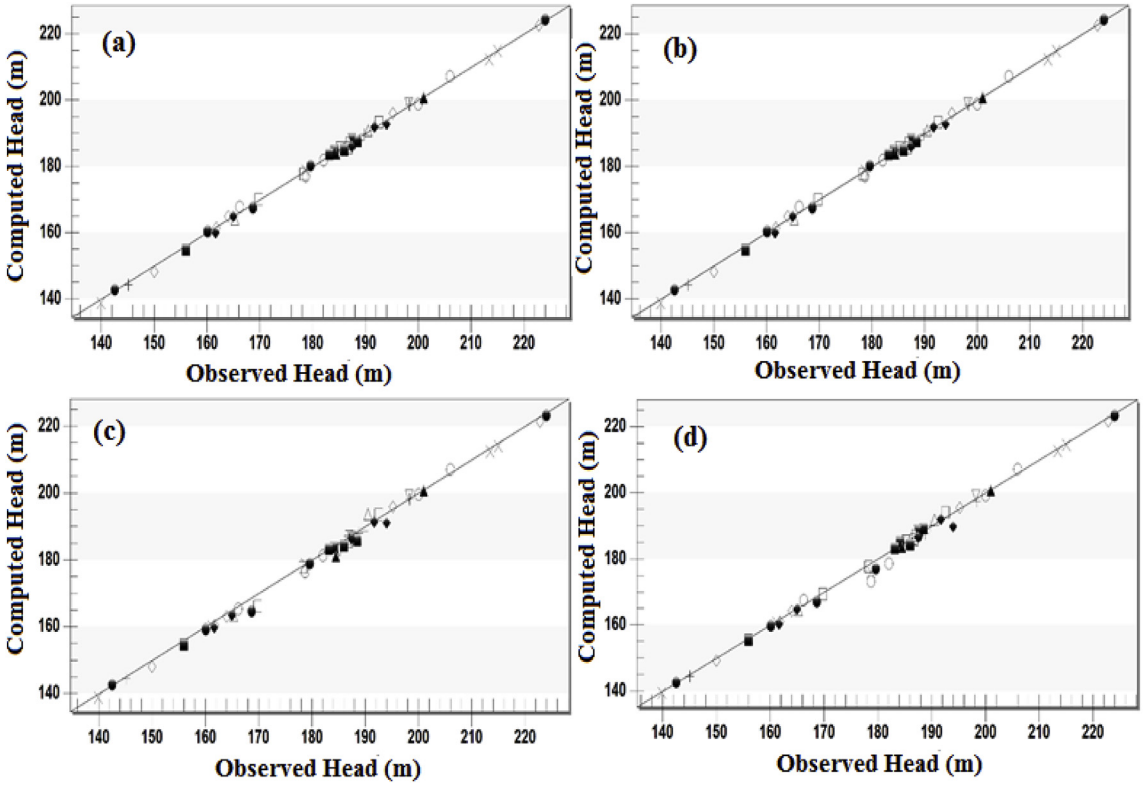

Fig. 17. Observed versus computed hydraulic head after (a) 10%, (b) 20%, (c) 40% and (d) 60% reduction in current recharge rate.

affect the entire ecosystem; causing land subsidence in some portions of the district, wiping-out some organisms and negatively affecting the livelihood of indigents.

It has been projected that predicted global changes in temperature and precipitation will modify regional climates and hydrologic systems. Predicted changes on meteorological variables such as temperature and rainfall can influence significant changes on aquifer recharge rates (Jyrkama and Sykes, 2007), which can lead to important aquifer head-level variations (Tall et al., 2012). Lemke et al. (2007) revealed that the global mean surface temperature has increased by 0.6 ± 0.2 °C since 1861, and predicts a rise of about 2–3 °C over the next century. Temperature rises, directly intensifies evaporation of surface water bodies and evapotranspiration of vegetation. As a result, these changes can impact precipitation amounts, periods and intensity rates, and in effect incidentally impact the flow and storage of water in surface and subsurface reservoirs such as groundwater aquifers.

In arid and semi-arid areas climate variability is expected to cause a decrease in groundwater recharge as a result of rising temperatures and increased evapotranspiration, as indicated by the stable isotope analysis in this study. As such a second scenario involved maintaining the increased abstraction rates, whilst progressively reducing the current recharge rate by 10%, 20%, 40% and 60%. This scenario sought to assess the hydraulic head levels and groundwater flow patterns in the wake of climate variability/change and its associated reduction in groundwater recharge.

When the groundwater recharge rate was gradually reduced by 10%, 20%, 40% and 60% of the current rate at calibration, the groundwater system only showed significant changes in drawdown and flow patterns, after 40% reduction in recharge at the current abstraction rate (Fig. 17). This suggest that the groundwater system can sustain current abstraction rates even in an instance where the recharge rate declined by up to 40% of the current rate. However, 60% reduction in the current recharge rate resulted in significant decline in hydraulic head and changes in flow patterns, with some portions of the district, mainly the central sections recording dry cells (Fig. 17d).

This observation therefore suggests that the underlying aquifer is significantly augmented by vertical groundwater recharge from precipitation and in an instance where climate change leads to decline in groundwater recharge by up to 40% of the current rate and abstraction rate increases as a result of demands associated with urbanisation and population growth by more than 100% of the current rate, the hydraulic heads would fall drastically to unsustainable levels and the general flow patterns will be completely modified.

Although it has been established in this study that the aquifer in the district is partly recharged by the White Volta river, however for the aquifer to sustain commercial abstractions beyond 100% of the current rate under conditions of reduced vertical recharge by more than 40% of the current rate, deliberate efforts such as ditches, farm ponds, contour bunds and so on would have to be made to enhance artificial vertical recharge to augment the natural recharge process so as to improve the availability of groundwater resources in the district.

5. Conclusion

The results of this study provide insight into the impacts of population growth and climate change on groundwater resources in the district, as well as estimates of hydraulic parameters of the aquifer underlying Talensi District. A steady state groundwater model has been calibrated for the crystalline aquifer of the district. The model reveals an apparent dominant northeast–southwest groundwater flow pattern influenced mainly by the hydraulic conductivity field of the district, with local flow systems which are controlled mainly by local variations in the topography. The flow patterns as revealed in this study is in conformity with findings of previous works in northern Ghana and in the Afram plains areas; which suggest that groundwater flow is structurally controlled by discrete entities oriented in northeast-southwest direction in line with the regional structural grain. The hydraulic conductivity in the district is highly variable and estimated to range between 0.001 and 58 m/day, which is consistent with the pumping test data and within ranges cited in literature for similar rocks. The high

variation in K is attributed to the various degrees of weathering and fracturing of the crystalline basement rocks underlying the district. Model calibration under steady state and CMB technique estimate average groundwater recharge to be 19.60 mm/year and 20.29 mm/year respectively which represents 2.00% and 2.07% of the annual precipitation of the district respectively. The relatively low recharge rates are associated with the low annual rainfall, low relative humidity, high temperatures reaching 45 °C and persistent high wind speeds which characterise the district, therefore resulting in evaporation of rain droplets in the course of the event and during infiltration, as revealed by stable isotope (δ^2H and $\delta^{18}O$) analysis. This is also consistent with the assertion by other researchers who worked in the area, suggesting that evaporation is an active process in groundwater at 3 m below the ground surface in some portions of the White Volta basin in northern Ghana.

Notwithstanding the low recharge rates, this study reveals that the aquifer is partly recharged by the White Volta River and holds good groundwater fortunes and promise for potential commercial groundwater development; as it can sustain increased abstractions by more than 100% of the current rate given that the current recharge rate is maintained. However, for the aquifer to sustain commercial abstractions beyond 100% of the current rate under conditions of reduced vertical recharge by more than 40% of the current rate, deliberate efforts such as ditches, farm ponds, contour bunds and so on would have to be made to enhance artificial vertical recharge to augment the natural recharge process so as to improve the availability of groundwater resources in the district.

Declaration of competing interest

None.

Acknowledgement

The authors are grateful to the Earth Science Department, University of Ghana for allowing the use of their isotope laboratory for this research. Authors also acknowledge the support of Prof. Dickson Adomako and Mr. Abass Gibrilla of Ghana Atomic Energy Commission for the valuable information they provided.

Appendix A. Supplementary data

Supplementary data associated with this article can be found, in the online version, at https://doi.org/10.1016/j.jafrearsci.2019.103665.

References

Abdul-Ganiyu, S., Gbedzi, V., 2015. Review of Existing Hydro Physical Properties on Soils, Flooding and Drought Trends on Ecosystem Services in Northern Ghana. pp. 36.
Addai, M.O., Yidana, S.M., Chegbeleh, L., Adomako, D., Banoeng-Yakubo, 2016. Groundwater recharge processes in the Nasia sub-catchment of the White Volta Basin: analysis of porewater characteristics in the unsaturated zone. J. Afr. Earth Sci. 4–14.
Afrifa, G.Y., Sakyi, P.A., Chegbeleh, L.P., 2017. Estimation of groundwater recharge in sedimentary rock aquifer systems in the Oti basin of Gushiegu District, Northern Ghana. J. Afr. Earth Sci. 131, 272–283. https://doi.org/10.1016/j.jafrearsci.2017.02.035.
Anderson, M.P., Woessner, W.W., 1992. Applied Groundwater Modeling: Simulation of Flow and Advective Transport. Academic Press, San Diego.
Aquaveo, 2018. Groundwater Modelling System, Version 10.2. Provo, Utah, USA.
Attandoh, N., Yidana, S.M., Abdul-Samed, A., Sakyi, P.A., Banoeng-Yakubo, B., Nude, P.M., 2013. Conceptualization of the hydrogeological system of some sedimentary aquifers in Savelugu–Nanton and surrounding areas, Northern Ghana. Hydrol. Process. 27, 1664–1676. https://doi.org/10.1002/hyp.9308.
Banoeng-Yakubo, B., Yidana, S., Ajayi, O., Anku, Y., 2010. Hydrogeology and groundwater resources of Ghana: a review of the hydrogeology and hydrochemistry of Ghana. In: Potable Water and Sanitation, pp. 77–114.
Bateni, S.M., Mortazavi-Naeini, M., Ataie-Ashtiani, B., Jeng, D.S., Khanbilvardi, R., 2015. Evaluation of methods for estimating aquifer hydraulic parameters. Appl. Soft Comput. 28, 541–549. https://doi.org/10.1016/j.asoc.2014.12.022.
Boateng, E.A., 1959. A Geography of Ghana. Cambridge University Press, Cambridge, UK.
Carney, J., Jordan, C., Thomas, C., McDonnell, P., 2008. A revised lithostratigraphy and geological map for the Volta Basin, derived from image interpretation and field mapping. In: Presented at the Voltain Basin, Ghana Workshop and Excursion. Geological Survey of Denmark and Greenland, Ghana, pp. 19–24.
Clark, I., Fritz, P., 1997. Environmental Isotopes in Hydrogeology. Lewis Publishers, USA.
Cooper, H.H., Jacob, C.E., 1946. A generalized graphical method for evaluating formation constants and summarizing well-field history. Eos Trans. Am. Geophys. Union 27, 526–534. https://doi.org/10.1029/TR027i004p00526.
Coplen, T.B., 1994. Reporting of stable hydrogen, carbon, and oxygen isotopic abundances. Pure Appl. Chem. 66, 273–276. https://doi.org/10.1016/0375-6505(95)00024-0.
Craig, H., 1961. Isotopic variation in meteoric waters. Science 133, 1702–1703. https://doi.org/10.1126/science.133.3465.1702.
CSIR-WRI, 2000. Climate Change Impacts on Water Resources in Ghana. 9964-85-419-6 Annual report No.
Dapaah-Siakwan, S., Gyau-Boakye, P., 2000. Hydrogeologic framework and borehole yields in Ghana. Hydrogeol. J. 8, 405–416. https://doi.org/10.1007/PL00010976.
Darko, E., 2015. Hydrogeological Characterization of the White Volta River Basin of Ghana. Unpublished MPhil thesis. University of Ghana, Accra.
Das, A., Maiti, S., Naidu, S., Gupta, G., 2017. Estimation of spatial variability of aquifer parameters from geophysical methods: a case study of Sindhudurg district, Maharashtra, India. Stoch. Environ. Res. Risk Assess. 31, 1709–1726. https://doi.org/10.1007/s00477-016-1317-4.
Domenico, P.A., Schwartz, F.W., 1990. Physical and Chemical Hydrogeology. John Wiley & Sons, New York.
EPA, 2008. Ghana initial national communication under the united nations framework convention on climate change. Accra, Ghana. Acts Commercial Ltd.
Fagariba, C.J., Song, S., Baoro, S.K.G.S., 2018. Climate change in Upper East Region of Ghana; challenges existing in farming practices and new mitigation policies. Open Agric. 3, 524–536. https://doi.org/10.1515/opag-2018-0057.
FAO, 2017. AQUASTAT: FAO's global information system on water and agriculture: E-agriculture. [WWW Document]. URL. http://www.fao.org/e-agriculture/news/aquastat-faos-global-information-system-water-and-agriculture accessed 8.27.19.
Gonfiantini, R., 1986. Environmental isotopes in lake studies. In: Fritz, P., Fontes, J.C. (Eds.), Handbook of Environmental Isotope Geochemistry. Elsevier, New York, pp. 113–168.
Gyau-Boakye, P., 2001. Sources of rural water supply in Ghana. Water Int. 26, 96–104.
Gyau-Boakye, P., Tumbulto, J.W., 2006. Comparison of rain- fall and runoff in the humid south-western and the semiarid northern savannah zone in Ghana. Afr. J. Sci. Technol. Sci. Eng. Ser. 7, 64–72.
Harbaugh, A.W., Langevin, C.D., Hughes, J.D., Niswonger, R.G., Konikow, L.F., 2017. MODFLOW-2005: USGS three-dimensional finite-difference groundwater model. U.S. Geological Survey.
Hill, M.C., Banta, E.R., Harbaugh, A.W., Anderman, E.R., 2000. MODFLOW-2000, the U.S. Geological Survey Modular Ground-Water Model; User Guide to the Observation, Sensitivity, and Parameter-Estimation Processes and Three Post-processing Programs (USGS Numbered Series No. 2000–184). Open-File Report. U.S. Geological Survey, Denver, CO.
Houston, J., 2007. Recharge to groundwater in the Turi Basin, northern Chile: an evaluation based on tritium and chloride mass balance techniques. J. Hydrol.
Junner, N.R., Hirst, T., 1946. The geology and hydrogeology of the Volta basin (vol.8 of memoir). Gold Coast Geol. Surv., Gold Coast.
Jyrkama, I.M., Sykes, J.F., 2007. The impact of climate change on spatially varying groundwater recharge in the grand river watershed. J. Hydrol. 338, 237–250.
Kesse, G.O., 1985. The Mineral and Rock Resources of Ghana. Balkema, Rotterdam.
Kortatsi, B.K., 1994. Groundwater utilization in Ghana. In: Proceedings of the Helsinki Conference on Groundwater Resources at Risk. Presented at the International Association of Hydrological Sciences, Wallingford, UK. International Association of Hydrological Sciences, IAHS Publ, Helsinki, Finland, pp. 149–156.
Kortatsi, B.K., Tay, C.K., Anornu, G., Hayford, E., Dartey, G.A., 2007. Hydrogeochemical evaluation of groundwater in the lower Offin basin, Ghana. Environ. Geol. 53, 1651–1662. https://doi.org/10.1007/s00254-007-0772-0.
Kyei-Baffour, N., Ofori, E., Mensah, E., Agyare, W., Atta-Darkwa, T., 2013. Modelling groundwater flow of the Besease inland valley Bottom in Ghana. Glob. J. Biol. Agric. Health Sci. 2, 52–60.
Lemke, P., Ren, J.F., B Alley, R., Allison, I., Carrasco, J., Flato, G., Fujii, Y., Kaser, G., Mote, P., Thomas, H.R., Zhang, T., 2007. IPCC, 2007. Climate Change 2007. Synthesis Report. Contribution of Working Groups I, II & III to the Fourth Assessment Report of the Intergovernmental Panel on Climate Change. IPCC, Geneva.
Lloyd's 360° Risk Insight, 2010. Global Water Scarcity, Risks and Challenges for Business.
Martin, N., 2006. Development of a Water Balance for the Atankwidi Catchment, West Africa–A Case Study of Groundwater Recharge in a Semi-arid Climate. Cuvillier Verlag, Göttingen, Germany.
Obuobie, E., Diekkrueger, B., Agyekum, W., Agodzo, S., 2012. Groundwater level monitoring and recharge estimation in the White Volta River basin of Ghana. J. Afr. Earth Sci. 71–72, 80–86.
Ophori, D., 1999. Constraining permeabilities in large-scale groundwater system through model calibration. J. Hydrol. 224, 1–20. https://doi.org/10.1016/S0022-1694(99)00083-9.
Pelig-Ba, K.B., 2010. Analysis of stable isotope contents of surface and underground water in two main geological formations in the northern region of Ghana. West Afr. J. Appl. Ecol. 15. https://doi.org/10.4314/wajae.v15i1.49430.
Picarro Inc, 2012. Picarro L2120-I Isotopic Water CRDS Analyser. Santa Clara, California, USA.
Saana, S.B.B.M., Fosu, S.A., Sebiawu, G.E., Jackson, N., Karikari, T., 2016. Assessment of the quality of groundwater for drinking purposes in the Upper West and Northern regions of Ghana. SpringerPlus 5. https://doi.org/10.1186/s40064-016-3676-1.

Slater, L., 2002. Electrical-hydraulic relationships observed for unconsolidated sediments. Water Resour. Res. 38, 1–13.
Subarna, D., Purwanto, M.Y.J., Murtilaksono, K., 2014. The relationship between monthly rainfall and elevation in the Cisankuy Watershed Bandung Regency. Int. J. Latest Res. Sci. Technol. 3, 55–60.
Talensi District Assembly, 2014. District Medium Term Development Plan under the Ghana Shared Growth and Development (Agenda) (Draft report 2014-2017). .
Tall, A., Mason, S.J., van Aalst, M., Suarez, P., Ait-Chellouche, Y., Diallo, A.A., Braman, L., 2012. Using seasonal climate forecasts to guide disaster management: the red cross experience during the 2008 west africa floods. Int. J. Geophys. https://doi.org/10.1155/2012/986016. 2012.
Todd, D.K., Mays, L.W., 2005. Groundwater Hydrology, third ed. John Wiley and Sons, Inc.
UNDP, 2019. Increasing Water Supplies in Rural Ghana | UNDP in Ghana. [WWW Document]. UNDP. http://www.gh.undp.org/content/ghana/en/home/presscenter/articles/2019/increasing-water-supplies-in-rural-ghana.html accessed 8.27.19.
UNEP, 2002. State of the environment and policy retrospective: 1972–2002. In: Global Environment Outlook 3: Past, Present and Future Retrospectives. USGS-United.
Wardrop, W.L., 1980. Final Hydrogeological Report for Drilling Programme, vols. 994–99 (CIDA/GWSC).
WRC, 2011. Executive Report on the State of Groundwater Resources of the Northern Regions of Ghana. Water Resources Commission of Ghana.
Yankey, R.K., Akiti, T.T., Osae, S.R., Fianko, J., Duncan, E.A., Amartey, O.E., Essuman, D.K., Agyemang, O., 2011. The hydrochemical characteristics of groundwater in the Tarkwa Mining area, Ghana. Res. J. Environ. Earth Sci.
Yidana, S., Banoeng-Yakubo, B., Akabzaa, T.M., 2010. Analysis of groundwater quality using multivariate and spatial analyses in the Keta basin, Ghana. J. Afr. Earth Sci. 58, 220–234. https://doi.org/10.1016/j.jafrearsci.2010.03.003.
Yidana, S.M., Abdul-Samed, A., Banoeng-Yakubo, B., Nude, P.M., 2011. Characterization of the hydrogeological conditions of some portions of the neoproterozoic voltaian Supergroup in northern Ghana. J. Water Resour. Prot. 03, 861–875. https://doi.org/10.4236/jwarp.2011.312096.
Yidana, S.M., Chegbeleh, L.P., 2013. The hydraulic conductivity field and groundwater flow in the unconfined aquifer system of the Keta Strip, Ghana. J. Afr. Earth Sci. 86, 45–52.
Yidana, S.M., Essel, S.K., Addai, M.O., Fynn, O.F., 2015. A preliminary analysis of the hydrogeological conditions and groundwater flow in some parts of a crystalline aquifer system: afigya Sekyere South District, Ghana. J. Afr. Earth Sci. 104, 132–139.
Yidana, S.M., Fynn, O.F., Chegbeleh, L.P., Loh, Y., Obeng, M.A., 2014. Analysis of recharge and groundwater flow in parts of a weathered aquifer system in Northern Ghana. J. Appl. Water Eng. Res. 2, 91–104. https://doi.org/10.1080/23249676.2014.954009.
Yidana, S.M., Fynn, O.F., Chegbeleh, L.P., Nude, P.M., Asiedu, D.K., 2013. Hydrogeological conditions of a crystalline aquifer: simulation of optimal abstraction rates under scenarios of reduced recharge. Sci. World J. 2013, 606375. https://doi.org/10.1155/2013/606375.
Yidana, S.M., Ophori, D., Banoeng-Yakubo, B., 2008. Hydrochemical evaluation of the voltaian system—the Afram plains area, Ghana. J. Environ. Manag. 88, 697–707. https://doi.org/10.1016/j.jenvman.2007.03.037.